Magnetic recording, and phase transitions in the fcc Kagomé lattice:

A two-part talk.

Martin Plumer Memorial University of Newfoundland

Part I.
Ferromagnetism.

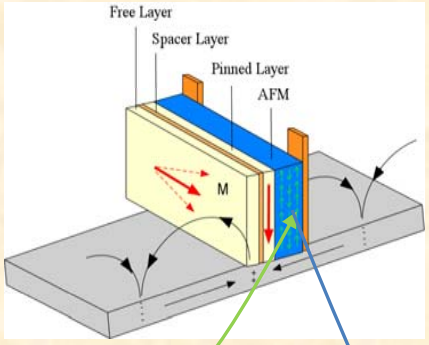

Exchange Pinning

Part II.
Antiferromagnetism

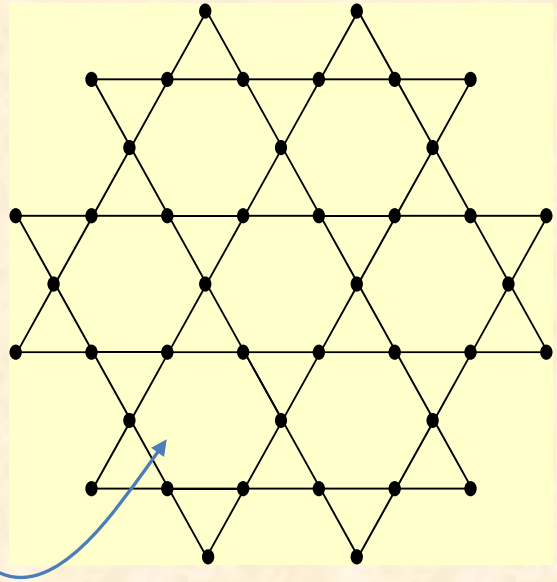

PART I. Review of Old and New Technologies in Magnetic Recording.

- Overview of *The Writer*, *The Reader* (Ir-Mn used for exchange pinning) and *The Media*.
- The Superparamagnetic Trilemma.
- The Recent: Perpendicular Recording and Dual-Layer ECC media.
- The Future (?): Many-layer ECC media, HAMR and BPM.

PART II. Monte Carlo Simulations *of ABC* stacked Kagomé planes.

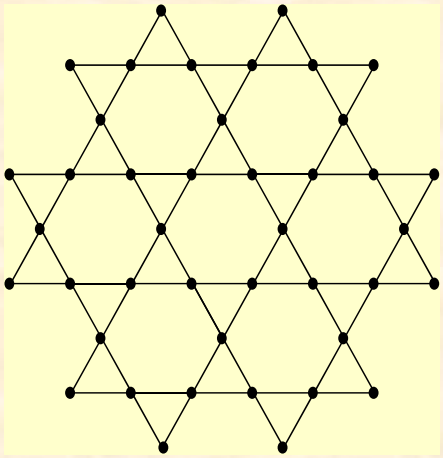

- Review of Exchange Pinning.
- $IrMn_3$ = fcc ABC stacked Kagomé lattice.
- XY and Heisenberg models with NN exchange (8 neighbors).
- Discontinuous transitions to LRO at finite T.
- Impact of spin degeneracies on sub-lattice order parameter.
- Case of weaker inter-layer coupling.
- Future simulations of exchange bias.

Areal Density Growth

- Additional innovations required at that point
  - heat-assisted recording
  - bit patterned media recording

Reduction in growth rate due to superparamagnetism

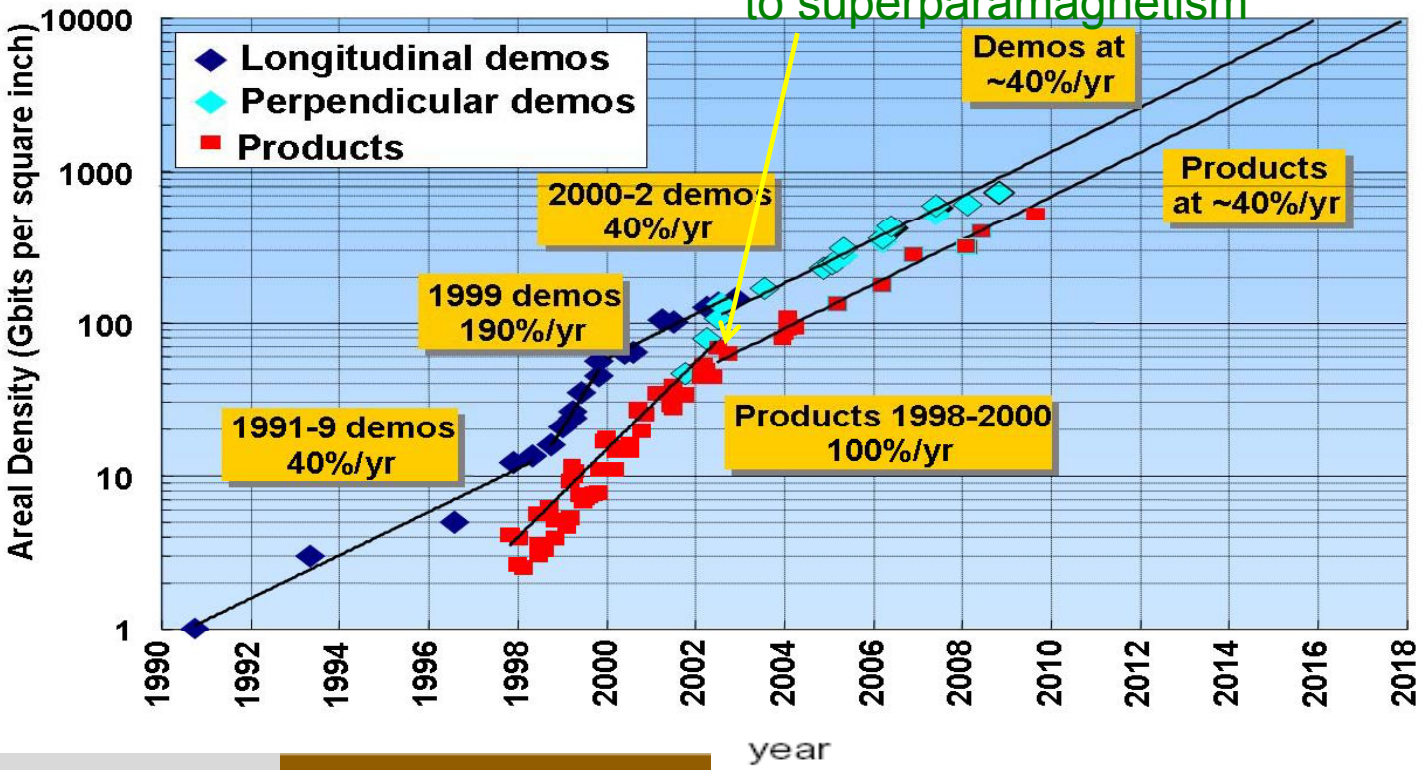

AD=(1/track width)*(1/bit length)
=(tracks per inch)(bits per inch)

- **Today: AD ~ 500Gb/in^2 Bit length ~ 2 media grains ~ 180 Å**
- **Tomorrow: AD ~ 1000Gb/in^2. Bit length ~ 1 media grain ~ 50 Å**

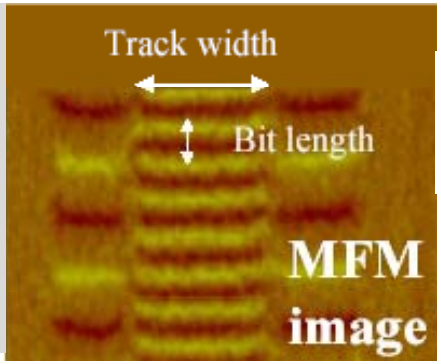

New Paradigms in Magnetic Recording, M.L. Plumer, J. van Ek, and W.C. Cain, Physics in Canada 67, 25 (2011)

The *three* elements of magnetic recording:
The Writer, The Reader, The Media.

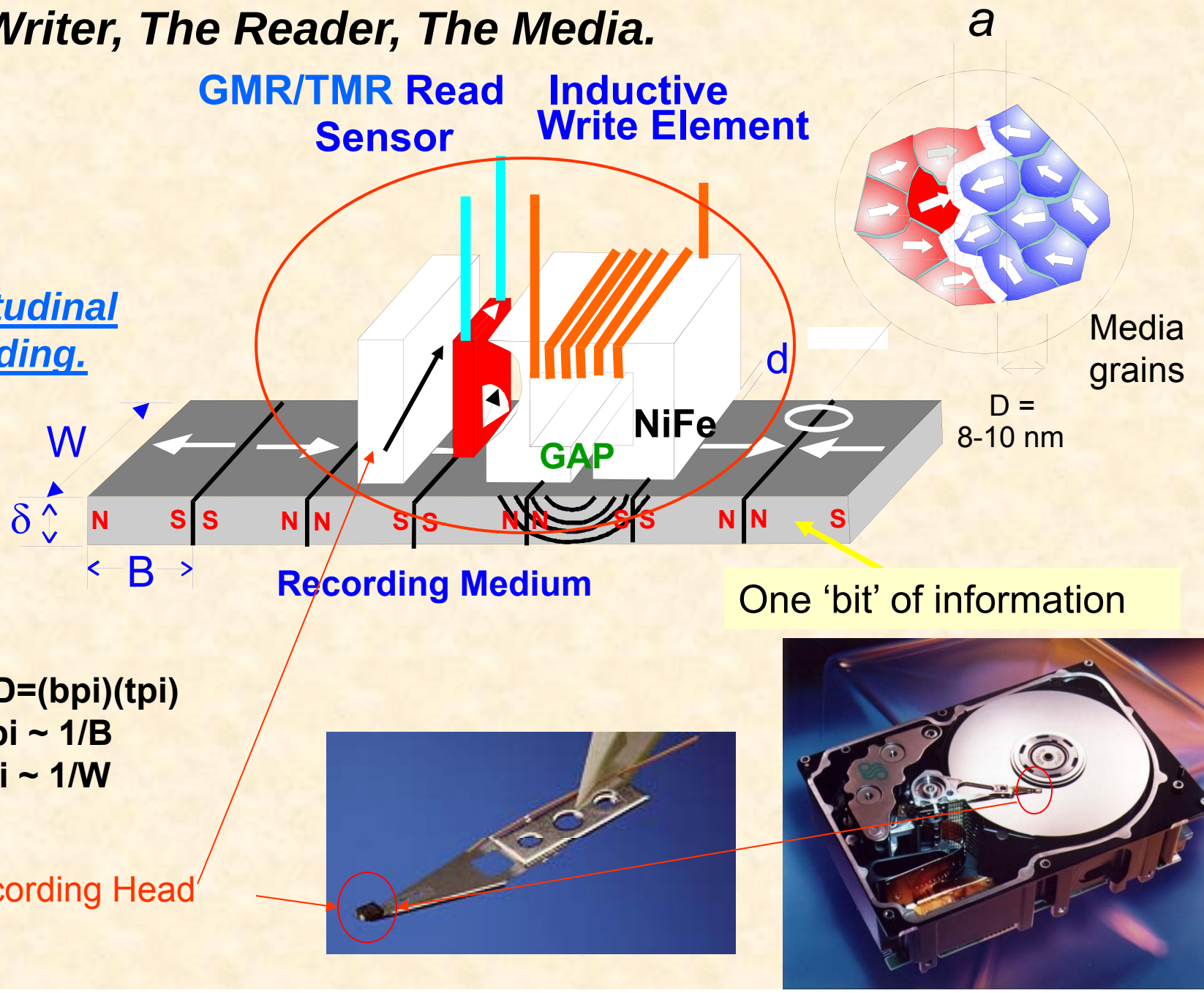

The HDD Head: Extreme Close-up

WD Production: 250 Gb/sq. in.

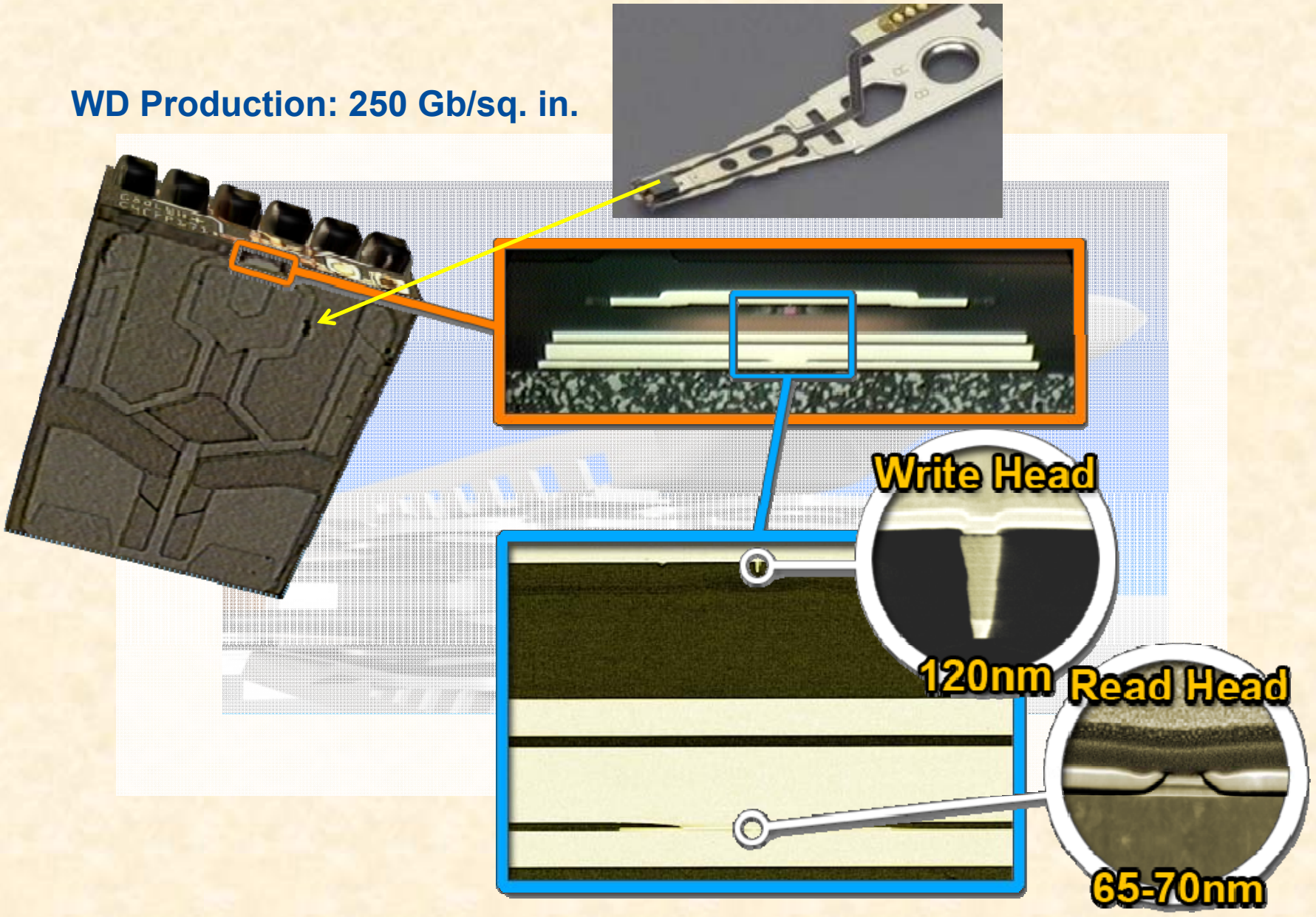

***The Writer*: Reversing the media magnetization**

Longitudinal Recording.

What's good for a write field profile.

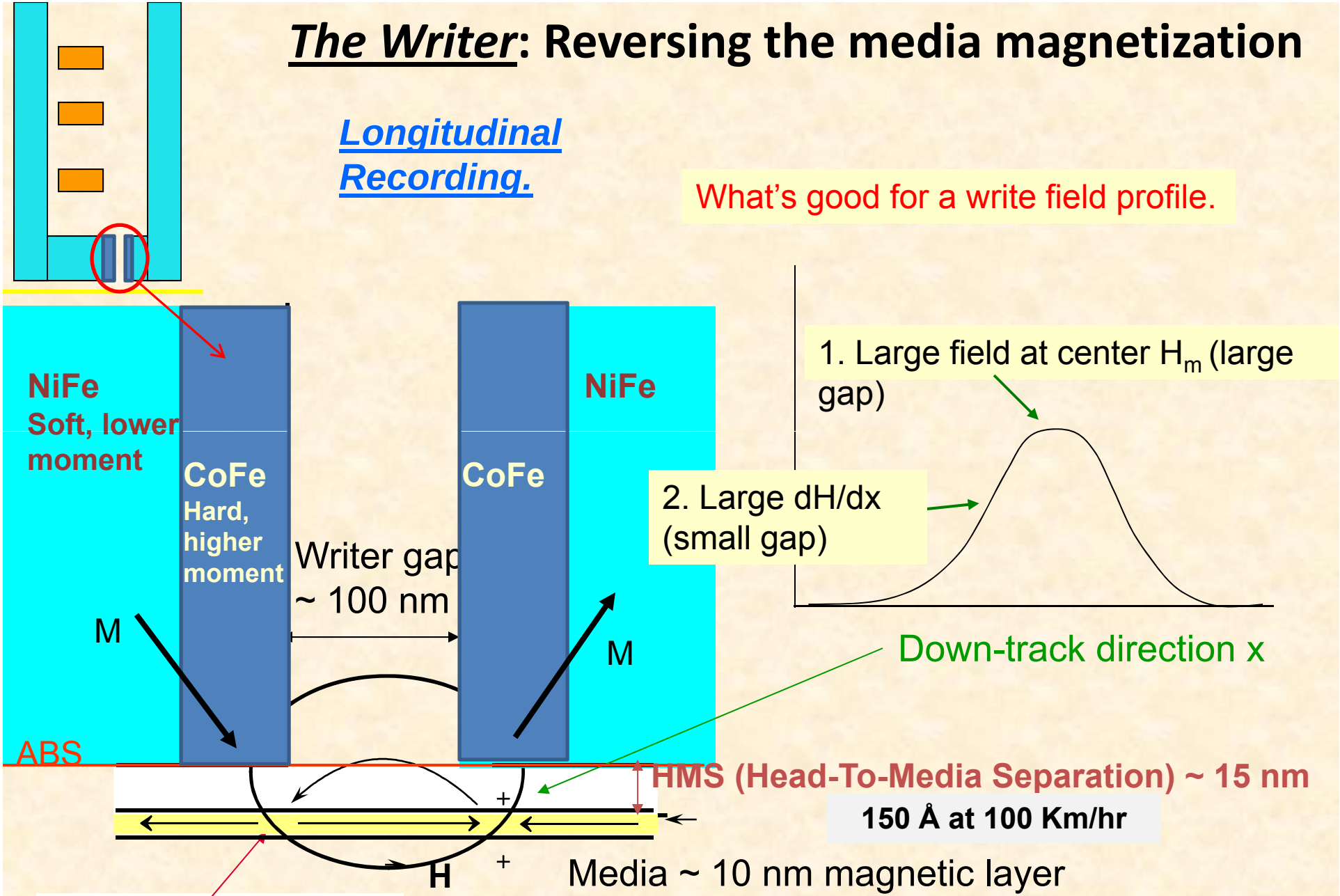

The Reader: Detection of media magnetization reversal.

GMR: 2007 Nobel Prize in Physics. Fert and Grünberg

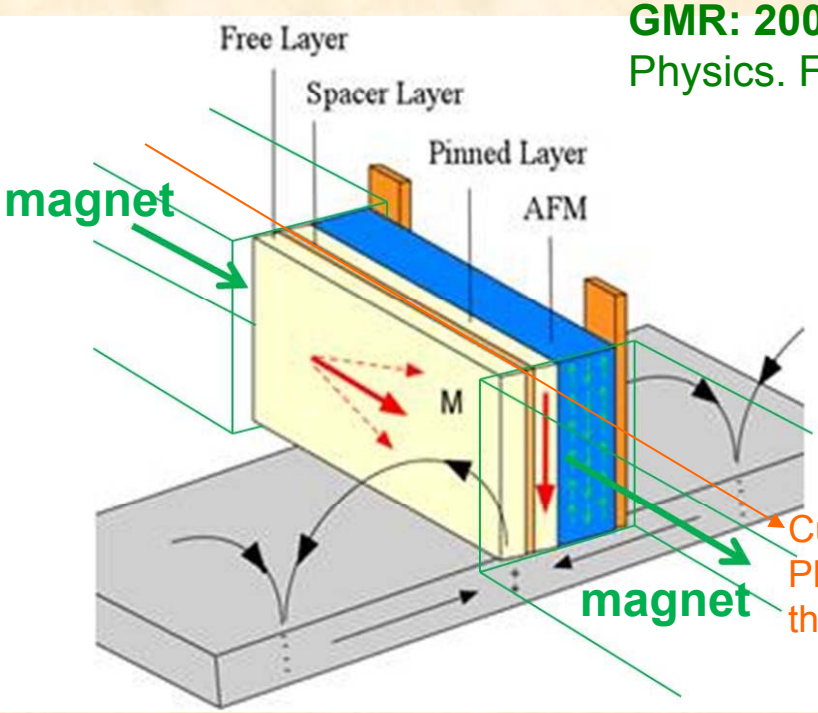

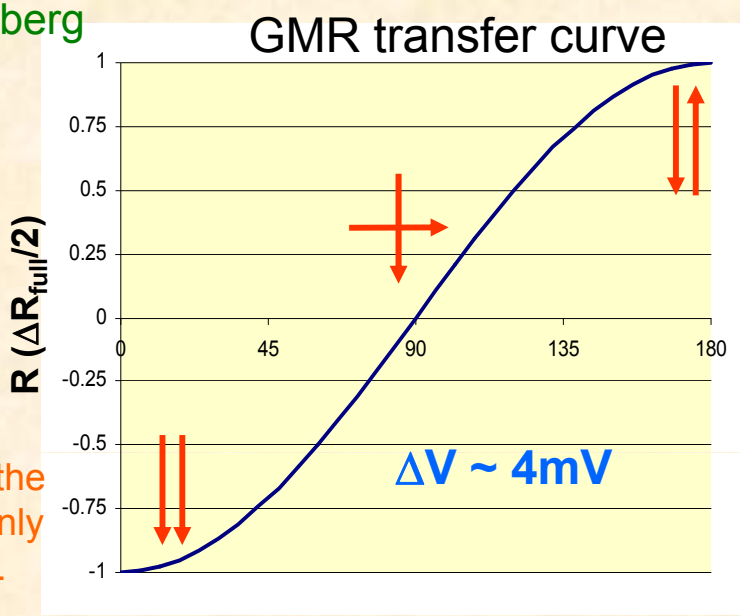

AFM = Ir-Mn (High T_N). 200 Å

media **PL = CoFe (big moment). 25 Å**

FL = $Ni_{80}Fe_{20}$ Permalloy 25 Å

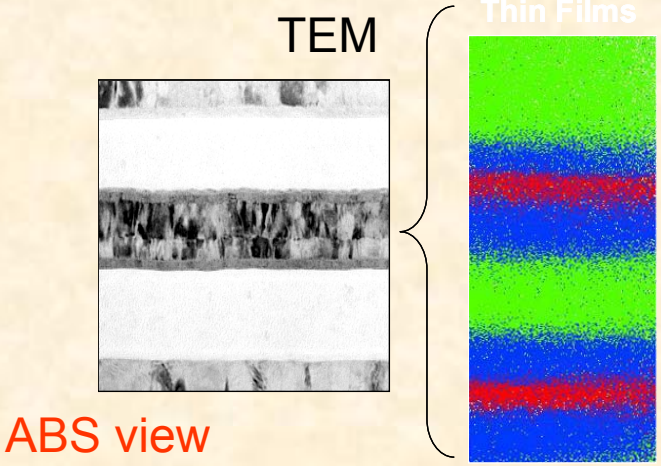

GMR effect involves surface and bulk scattering of spin polarized electrons between the Free Layer and Pinned Layer.

The Media: A "hard" granular magnet

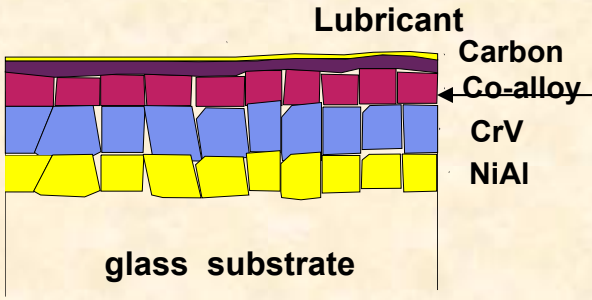

CoCrPt

longitudinal

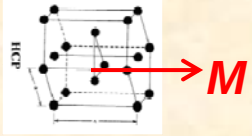

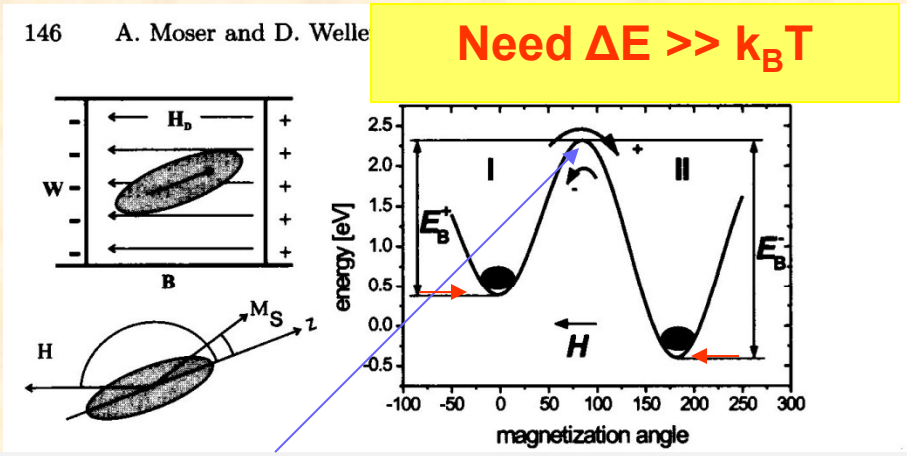

Need ΔE >> k_BT

Grain size ~ 16 nm

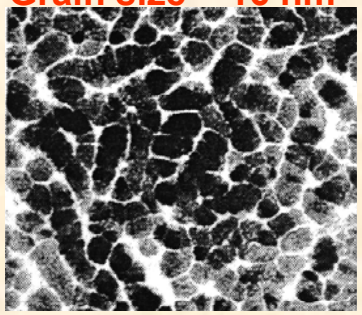

1 Gbit/in^2 media

Grain size ~ 9nm

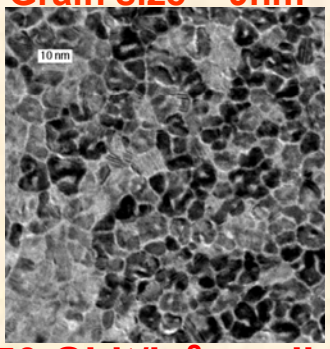

50 Gbit/in^2 media

ΔE = (crystal anisotropy)(grain volume = K*V

Switching Field ~ H_c=2K/M_s

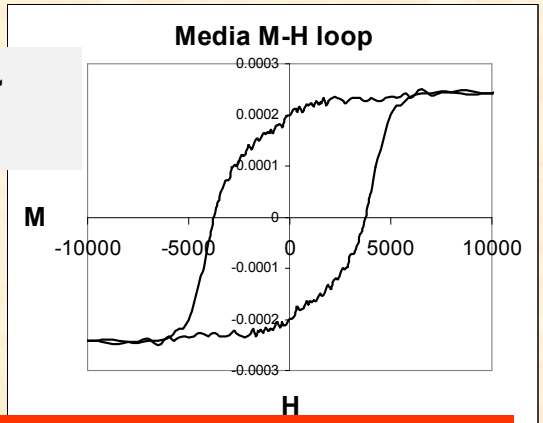

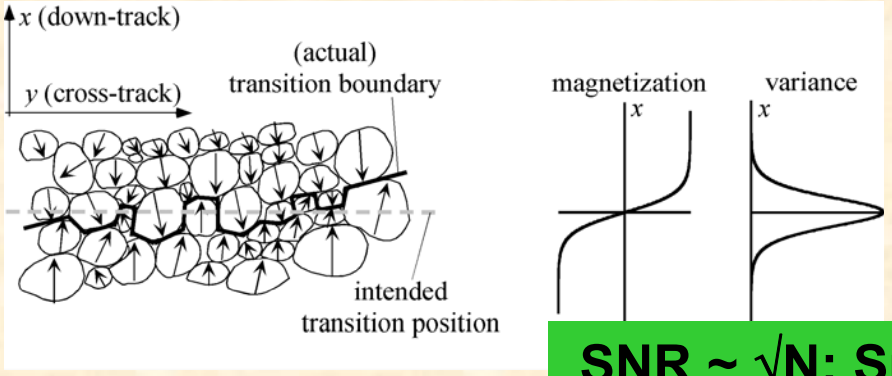

SUPERPARAMAGNETISM: Smaller grains are *worse* for thermal stability ('thermal idiots').

SNR ~ √N: Smaller grains are *better*.

The Trilemma **of shrinking dimensions.**

1. Smaller bits require smaller media grains to maintain SNR.
2. Smaller grains require larger anisotropy (energy barrier) to maintain thermal stability.
3. Larger anisotropy requires larger write fields to switch media transitions.

- Also: Smaller dimensions lead to less responsive read elements (magentically).
- Larger write fields require large moment materials to put at the business end of the write element.
- CoFe at 2.4 Tesla is the largest moment material stable at room temperature ***and has been used since 1999***.

Micromagnetic Modelling **of the spin valve response to a media transition field.**

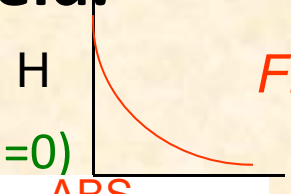

Field from media transition decays quickly

Quiescent state (H=0)

Response to field from a media

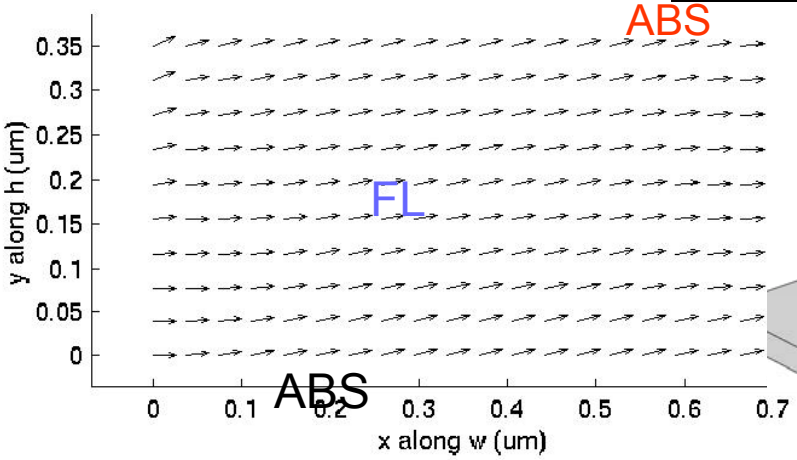

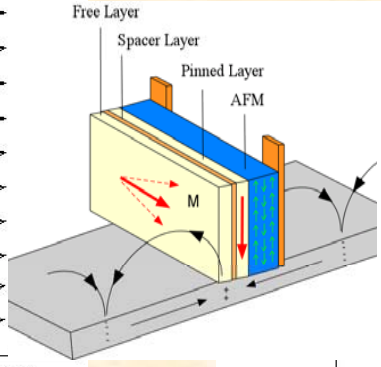

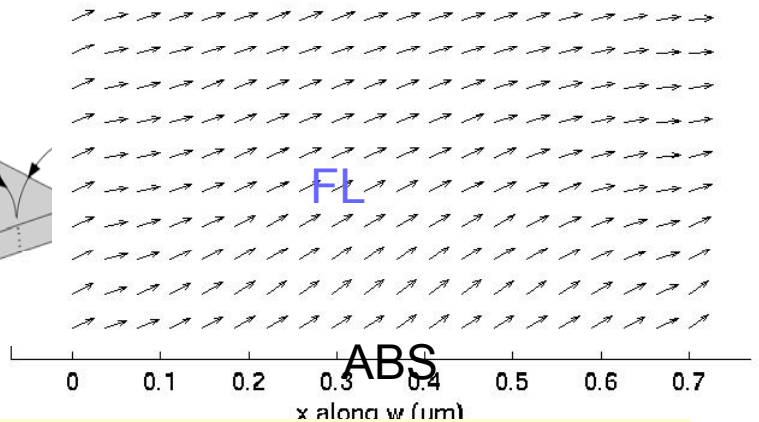

Shape anisotropy limits response for smaller devices.

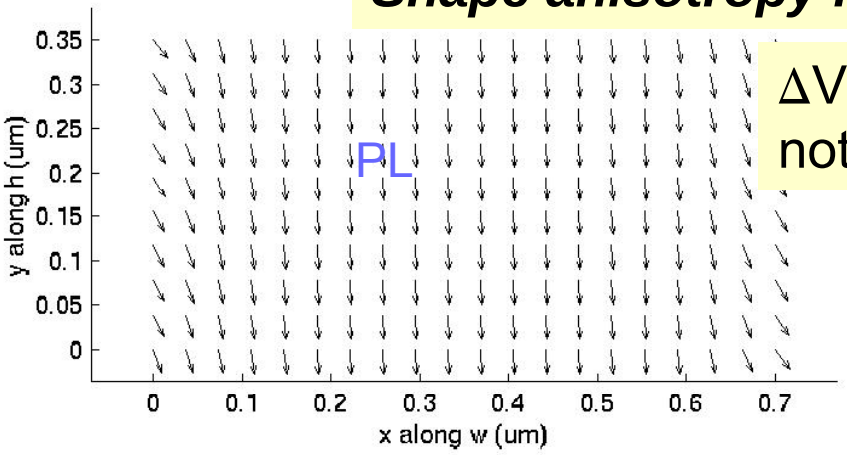

ΔV=1mV,
not 4mV.

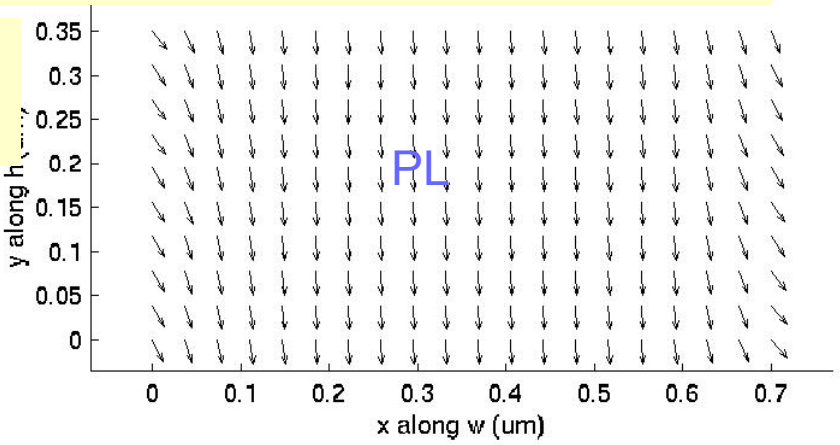

Micromagnetics: Reader Efficiency vs Sensor Height.

100% efficiency = full 180^0 rotation

22% efficiency →

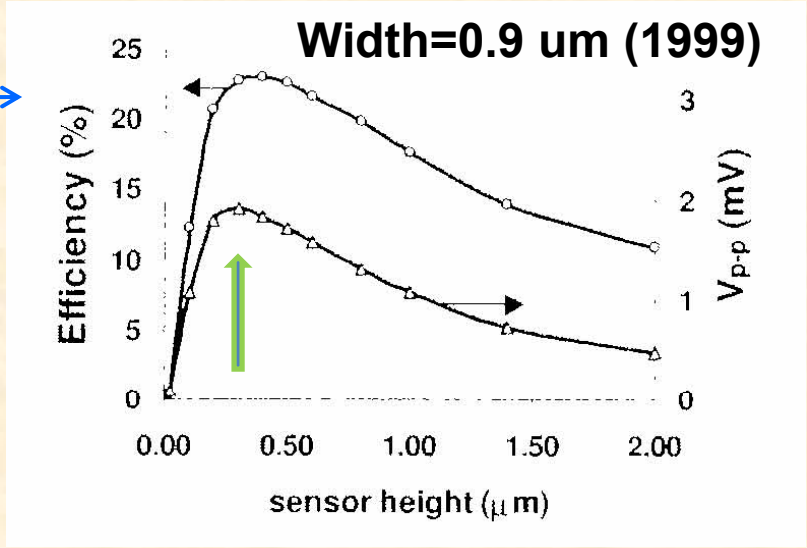

Present reader widths ~ 50 nm

Maximum efficiency for Height/Width ~ 1/3

The Physics of Ultra-High-Density Magnetic Recording, eds. M. L. Plumer, J. Van Ek, and D. Weller (Springer 2001).

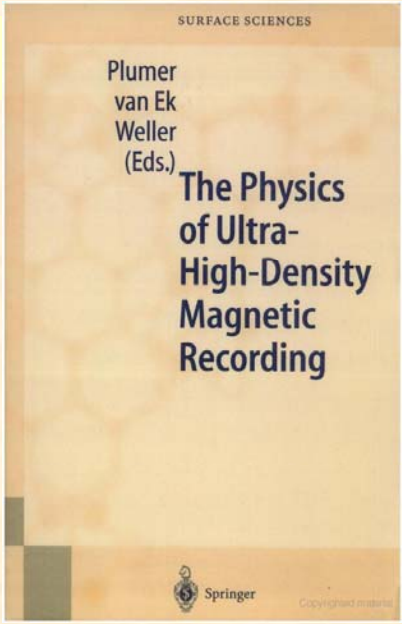

Micromagnetics of Medium Orientation Effects

Orientation Ratio (OR) accounted for by assuming a Gaussian distribution for the media *grain anisotropy axes direction* $\mathbf{H_K}$: mean and Standard Deviation.

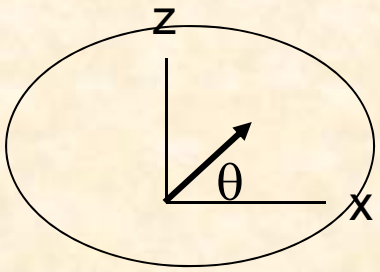

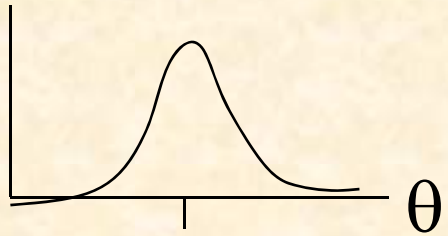

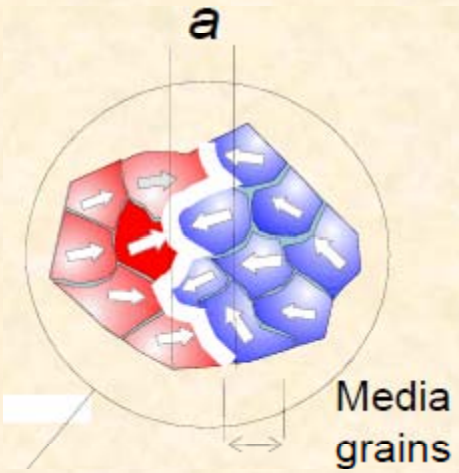

Isotropic media – very large standard deviation.

Oriented media – smaller standard deviation (SD).

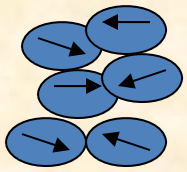

Expect better performance for media with a preference for **M** to lie in the down-track direction.

100Gb/in^2. Recorded tracks at high kbpi much improved with oriented media.

Isotropic media. 290 and 640 kbpi.

Oriented media. 640 kbpi.

OR ~ 1/SD

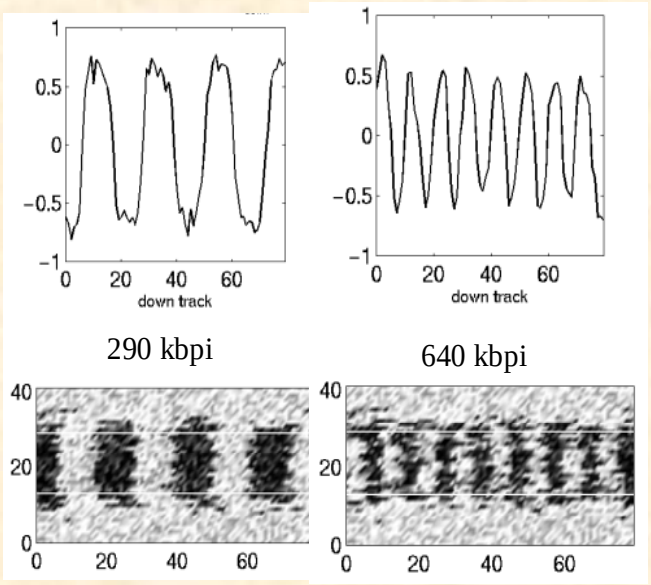

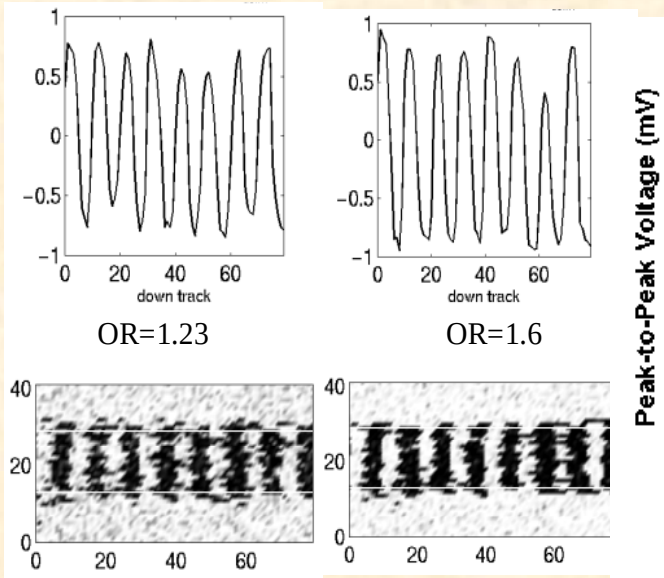

Amplitude vs OR

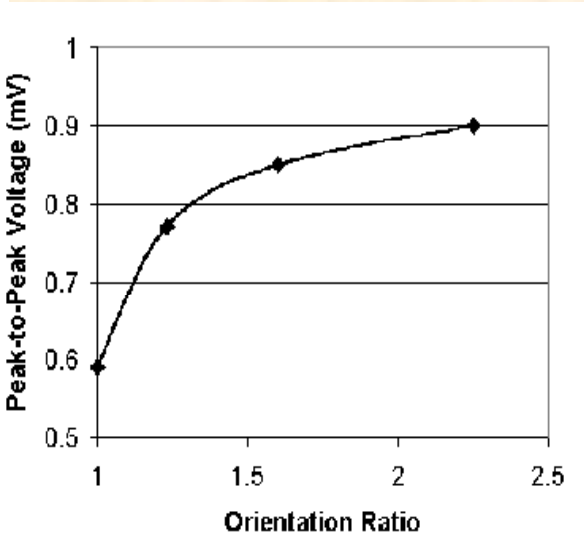

A clear message was received by recording media development groups. Highly oriented media is now the industry standard.

Perpendicular Recording: The ultimate in control of anisotropy-direction distributions

Longitudinal Recording

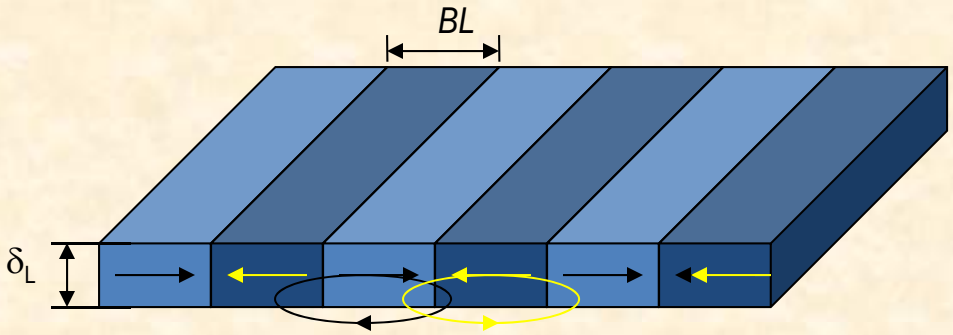

Magnetostatic fields destabilize the transitions (superparamagnetism).

Perpendicular Recording

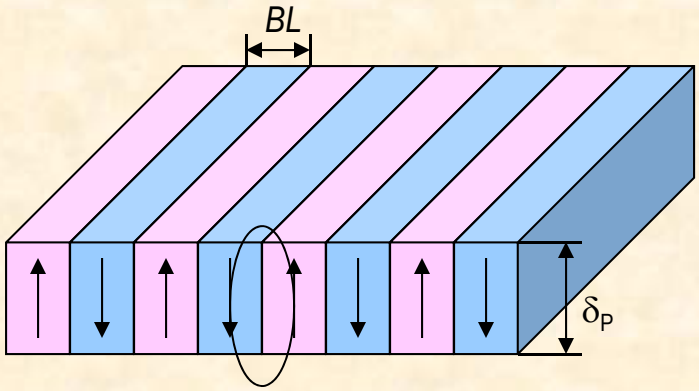

Magnetostatic fields stabilize the transitions.

Cobalt

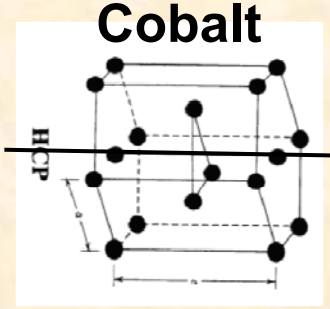

Anisotropy axis in plane

Hard to control distributions

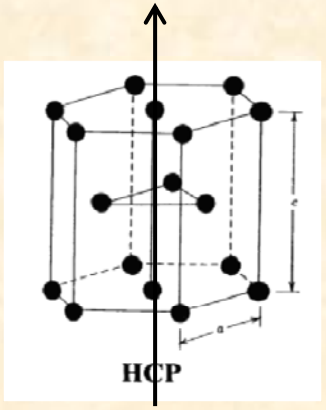

Anisotropy axis out of plane

Easier to control

Larger Write Fields due to media soft underlayer.

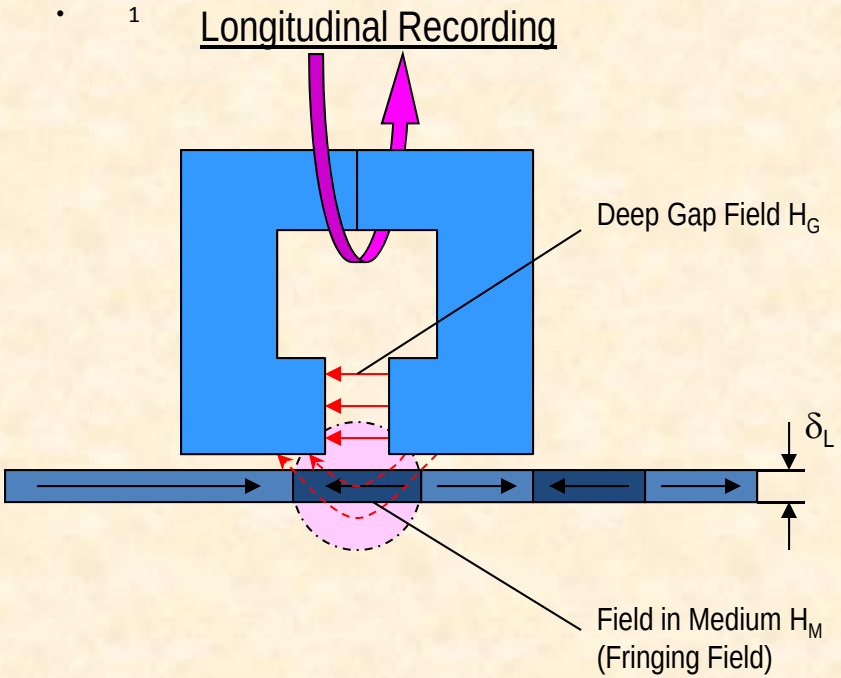

Single layer medium (longitudinal or perpendicular):

- *Transition is recorded by fringing field*

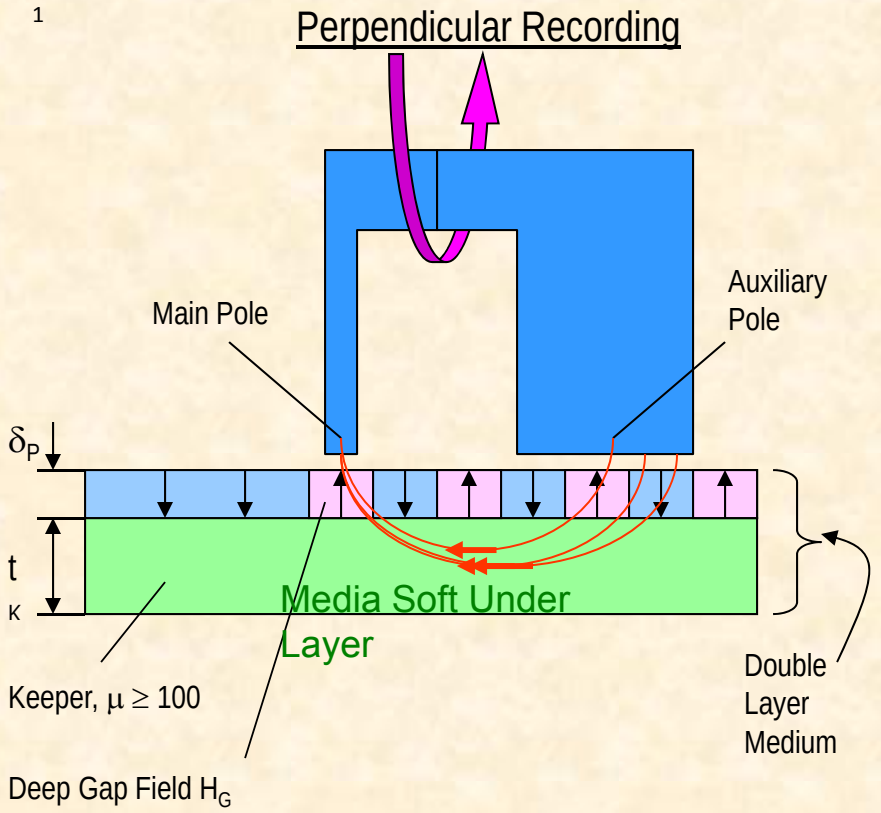

Double layer perpendicular media with soft magnetic Underlayer: media becomes part of the write element

- *Transition is recorded by deep gap field: 50 % boost.*

…and more field emanating from media transitions

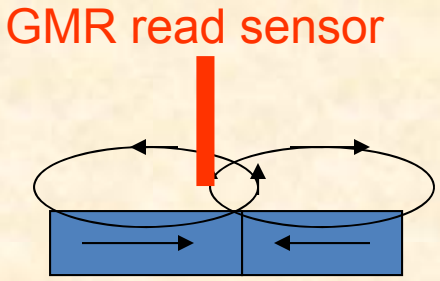

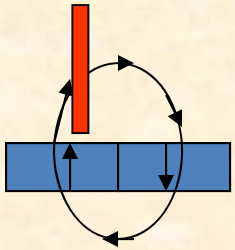

Stronger fields from perpendicular bits = larger play-back amplitude.

Another ~50% boost.

And TMR…Tunneling GMR Heads:

Double the read-sensor amplitude.

- **New Structure** (aka: MTJ, SDJ,Tunnel valve, spin tunneling head)
- **New materials**
- **New physics**

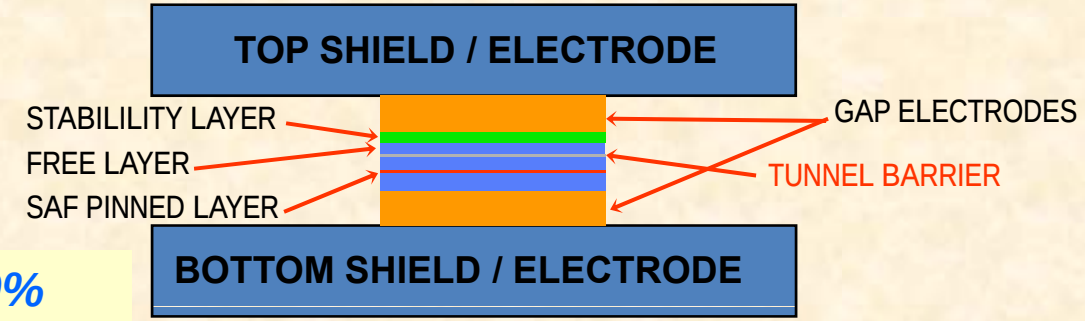

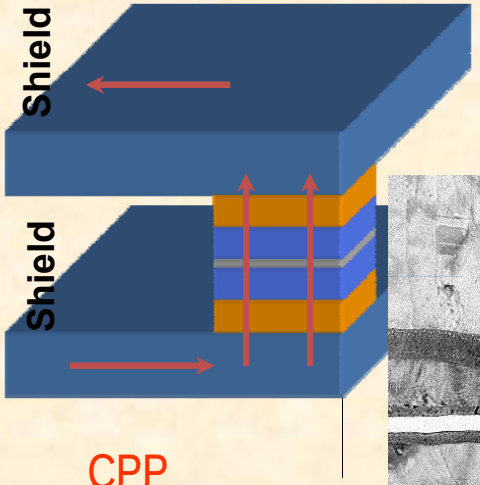

Another 50% boost in amplitude.

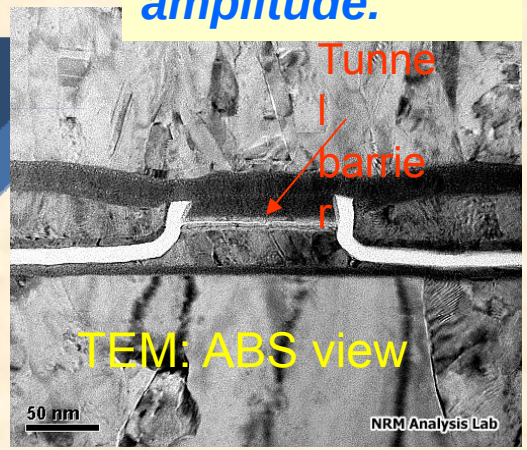

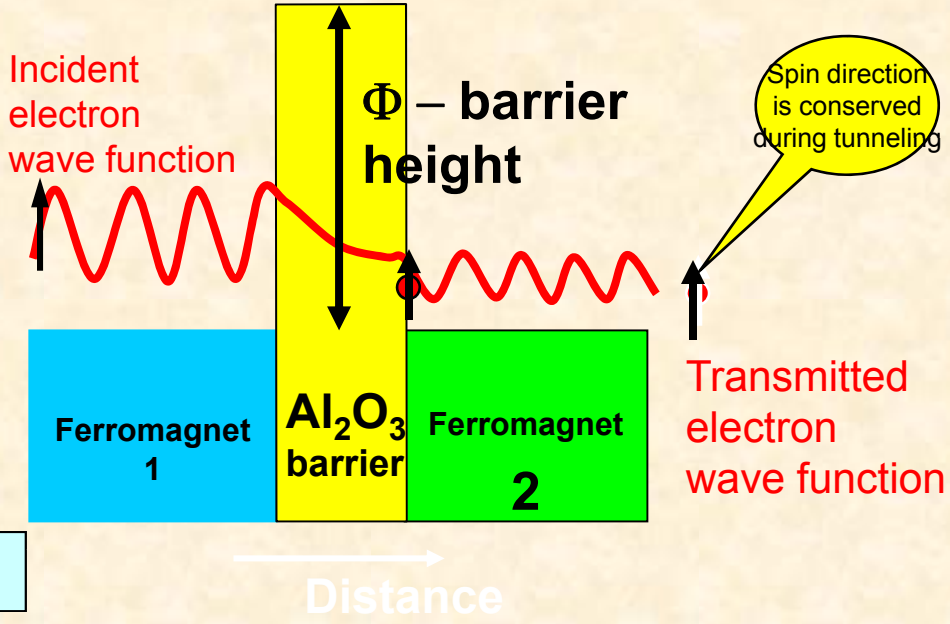

CPP = Current Perpendicular to Plane

Exchange-Coupled-Composite Media:

Easier to reverse with same thermal stability.

Gerardo BERTERO Western Digital Corporation

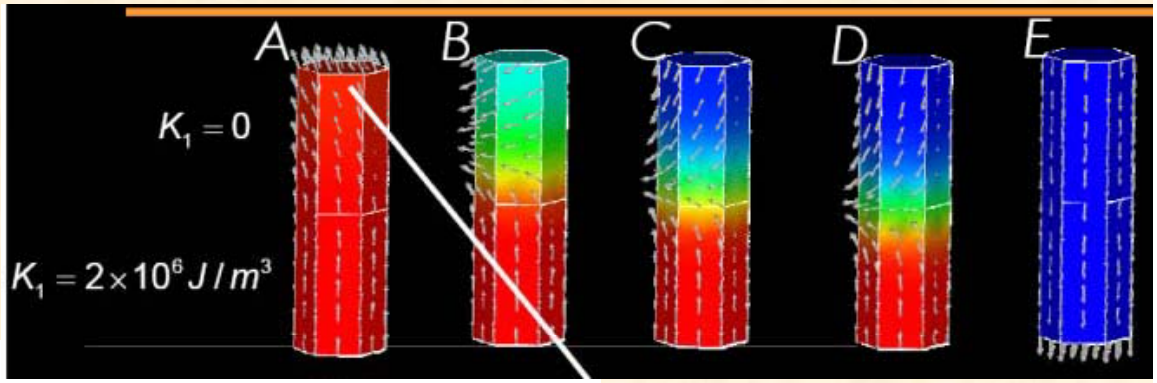

Introduction to ECC media

Material with extremely high anisotropy Ku and volume V_{hard}. Store information. Provide thermal stability

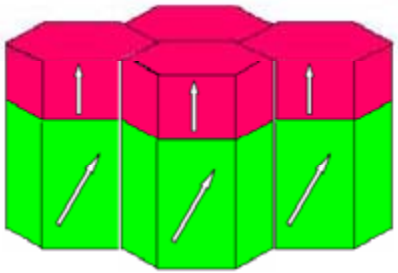

Soft material with volume V_{soft}. Facilitate switching of the grain.

$$\xi = \frac{2\Delta E}{M_s H_s V} \qquad K_u x V_{hard}$$

$$\frac{(M_{hard}V_{hard} + M_{soft}V_{soft})}{V_{hard} + V_{soft}} \qquad V_{hard} + V_{soft}$$

This term can be used to compare the switching fields of different kind of media with the same thermal barrier, volume and magnetization

UNIVERSITY OF MINNESOTA

Figure of merit:
Ratio of thermal energy barrier to switching energy.
ξ = 1 for single-layer
ξ = 2 for dual-layer

R.H. Victora and X. Shen, *IEEE Magnetics* ***41,*** *537-542 (2005).*

D. Suess *et al., J. Magn. Magn. Mat.* ***551,*** *290-291 (2005).*

Now What ?

Try more: Multi-Layer ECC Media

Gerardo BERTERO Western Digital Corporation

Advanced ECC Media

Concept:

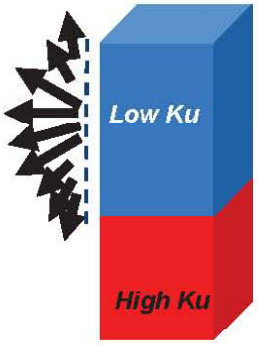

Figure of merit = 2

Practice:

Two-Spin Model

$$H_c = \frac{1}{4} \times \frac{2K_H}{J_{hard}}$$

Single EBL

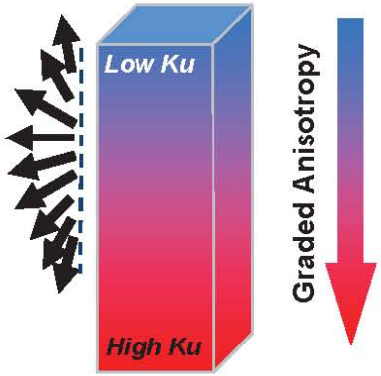

Figure of merit > 4

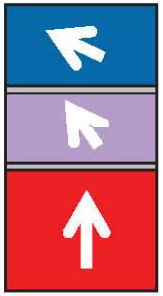

Three-Spin Model

$$H_c = \frac{1}{C} \times \frac{2K_H}{J_{hard}}$$

Double EBL

C>4

Try exotic. HAMR – Heat Assisted Magnetic Recording

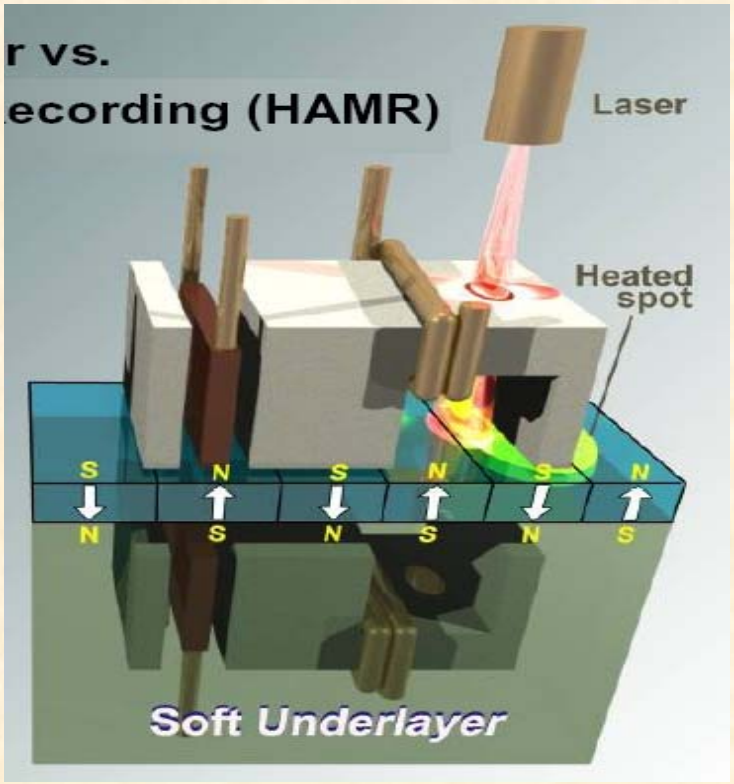

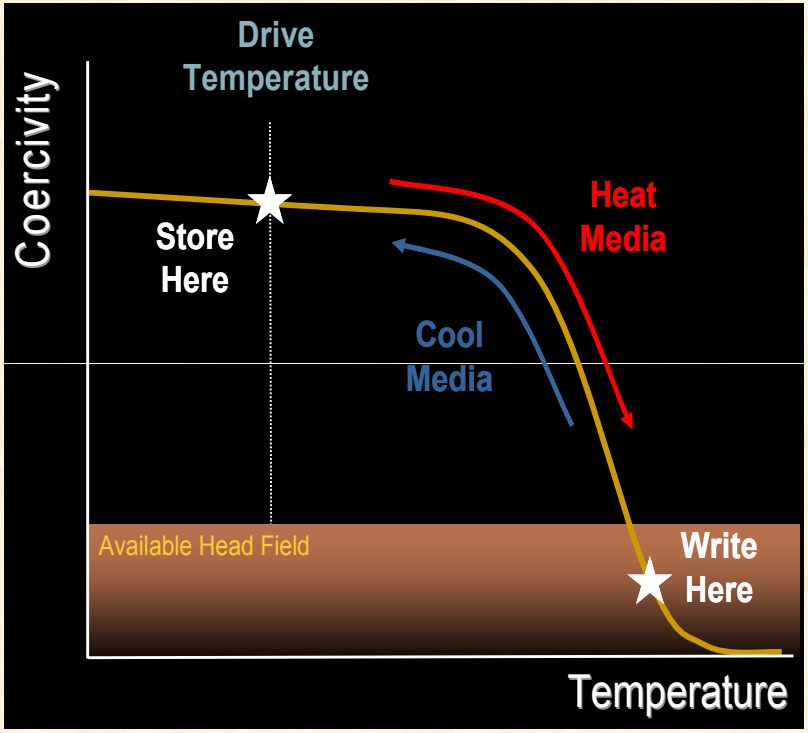

- The challenge in making HAMR work is in creating sufficiently small spatial thermal gradients that will prevent interference between adjacent bits.

Modeling HAMR at the atomic scale using LLG.

J.I. Mercer, M.L. Plumer, J.P. Whitehead, and J. Van Ek, Appl. Phys. Letts. 98, 192508 (2011).

Each grain = 2000 'spins'

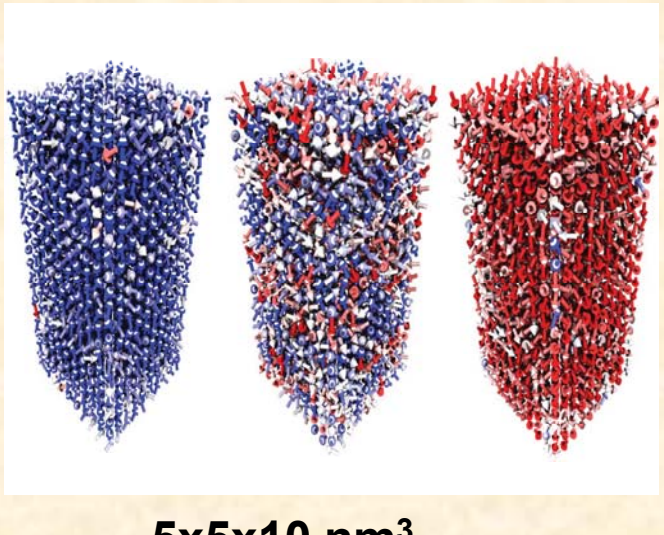

5x5x10 nm³

Grain reversal is highly non-uniform.

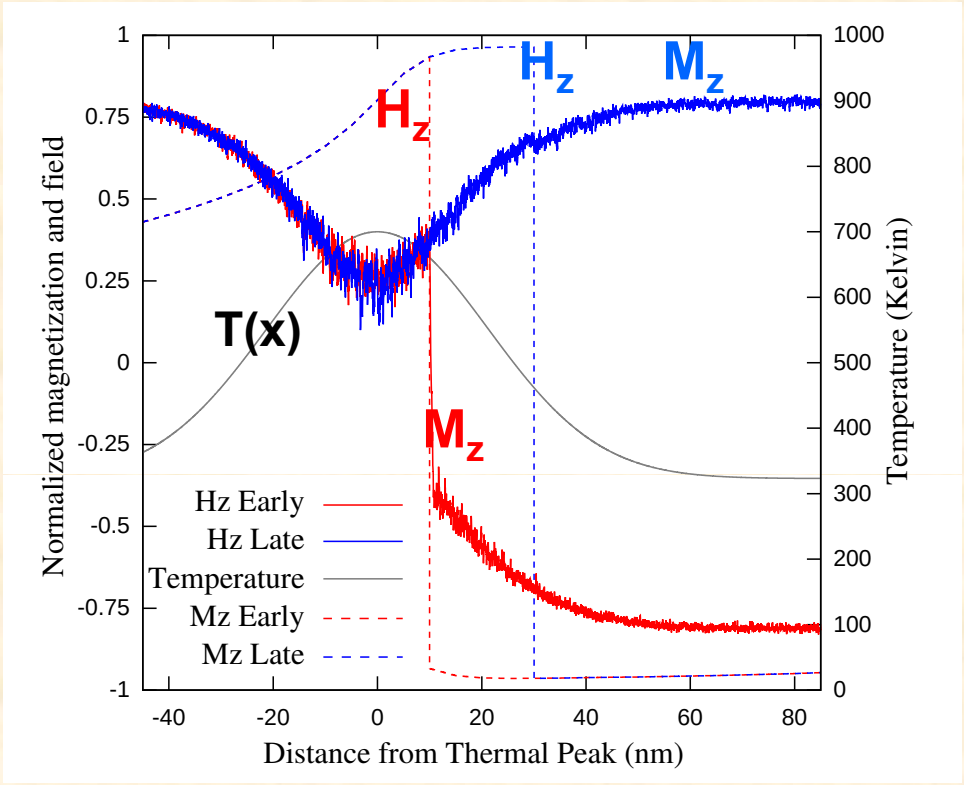

X = Down track direction

Position of temperature pulse relative to head field maximum is crucial.

Challenges.

- **Control of thermal spot size.**

Try more control:

Bit Patterned Media

Lithographically Patterned Bits:

One bit = one magnetic grain to decrease transition jitter and increase SNR.

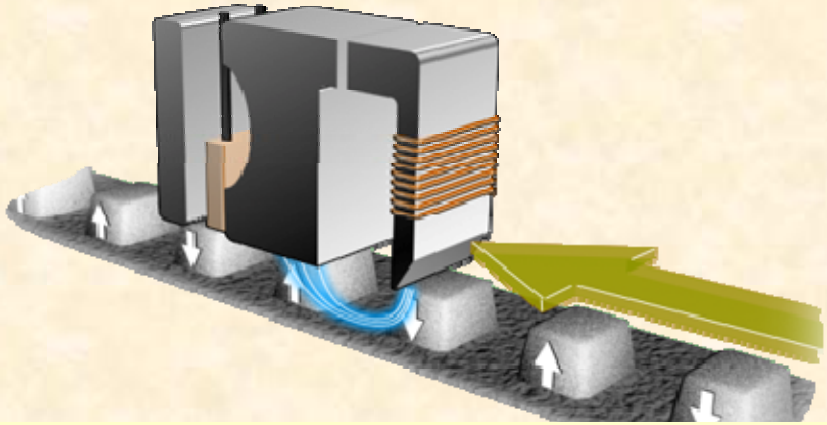

Challenges.

- **Making them small enough (1 Tb/in^2 $\Longrightarrow$ 13 nm bits).**
- **Finding the bits for write and read.**

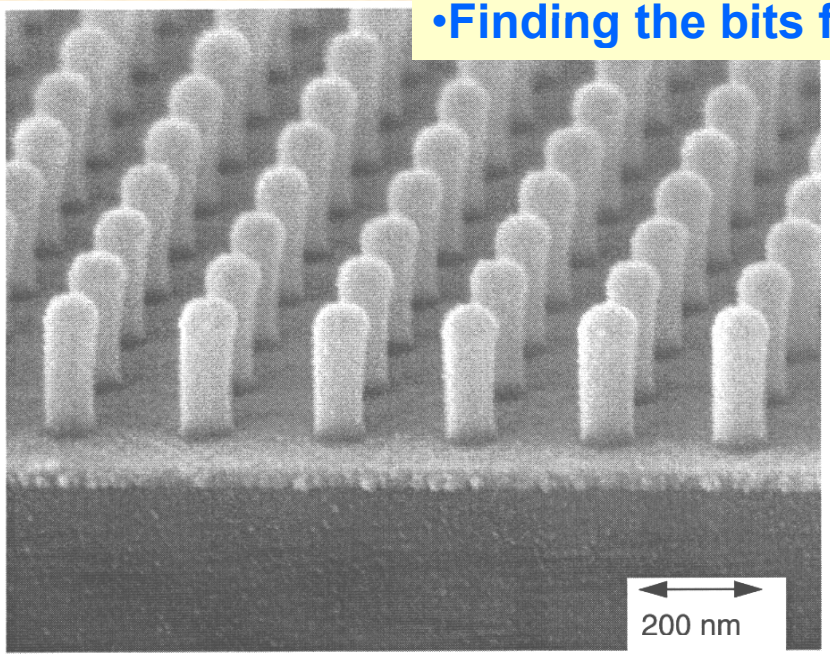

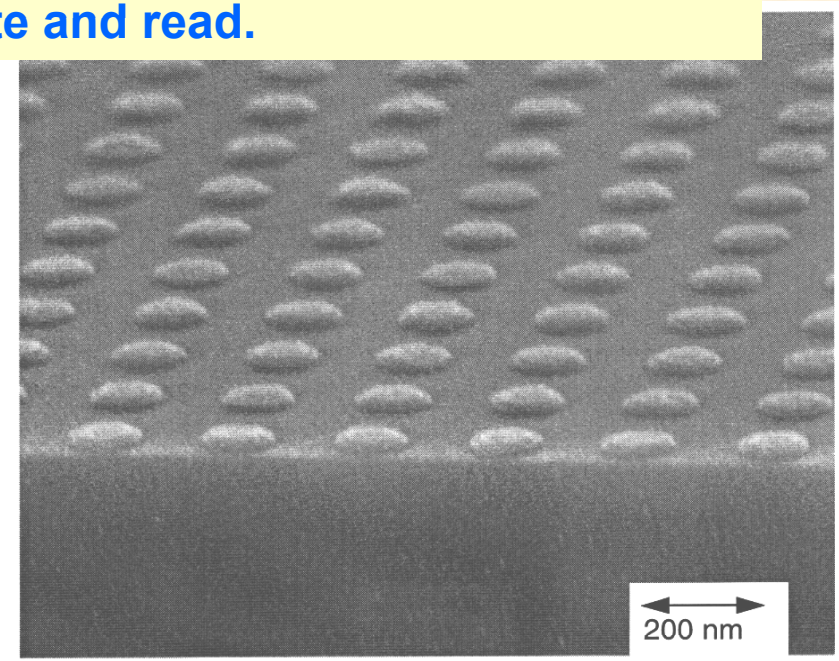

100 nm diameter Co/Cu bilayer dots with 200 nm period

Conclusions (Part I)

- Large number of new technologies introduced into magnetic recording over the past decade: GMR, Perpendicular, TMR, ECC,…

- New paradigms such as HAMR or BPM will be very challenging to implement effectively.

- Most likely advances in *Areal Density* in the near future will come from materials science and increased understanding of the underlying physics through numerical simulations.

Seagate HAMRs hard drives to 1Tb per square inch
Published on 20th March 2012 by Gareth Halfacree
Seagate's HAMR-based hard drives could, it claims, store up to 60TB of data before the technology reaches its upper limit.
Storage giant Seagate has become the first hard drive manufacturer to reach the dizzy heights of one terabit per square inch areal density, using a technology known as heat-assisted magnetic recording (HAMR.)

Designed as a next-generation replacement for perpendicular magnetic recording as used in today's hard drives, HAMR holds the potential for 3.5in hard drives holding as much as 60TB. That, Seagate is quick to point out, would mean more bits in a square inch of hard drive platter than stars in the Milky Way.

PART II.

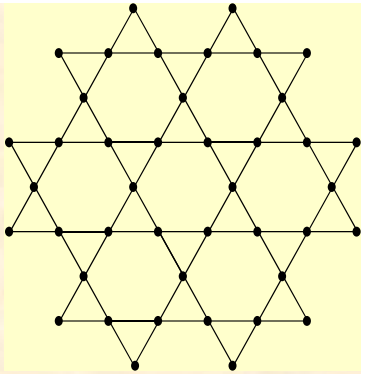

Monte Carlo Simulations of *ABC* stacked Kagomé planes.

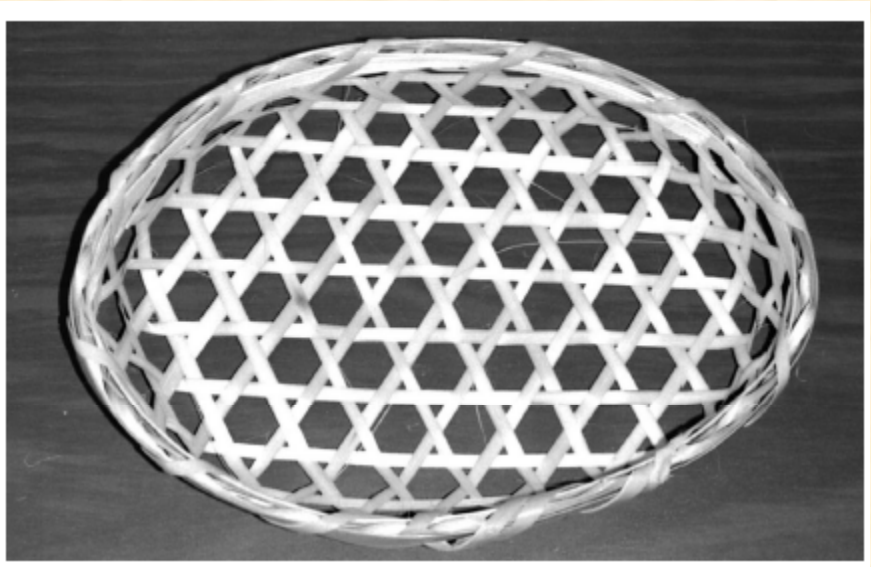

Kagome: The Story of the Basketweave Lattice. M. Mekata, Physics Today Feb. 2003.

First study of magnetic properties: I. Syozi, Prog. Theor. Phys. (1951).

Ir-Mn ($IrMn_3$) most popular AF material in spin valves.

$IrMn_3$ = fcc $AuCu_3$ crystal structure. Also: $RhMn_3$ and $PtMn_3$

I. Tomeno et al J. Appl. Phys. 86, 3853 (1999).

Ir (non-magnetic)

Mn

***Ordered* Phase**

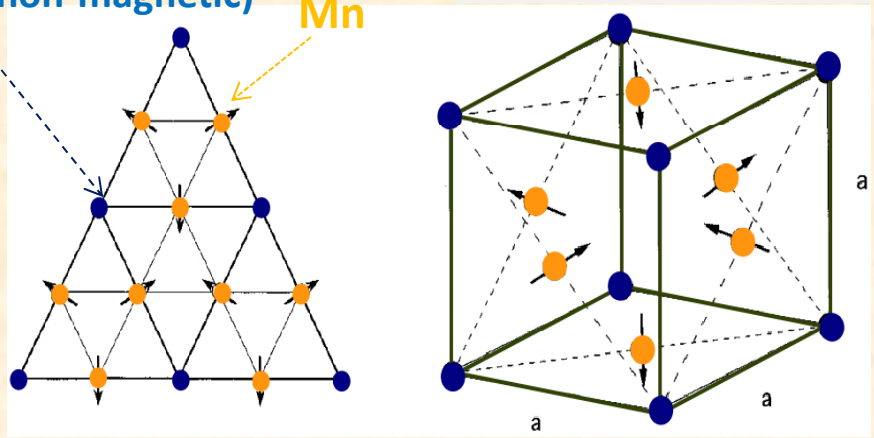

'T1' ⇒ 2D spin structure

Neutron diffraction on bulk single crystals.

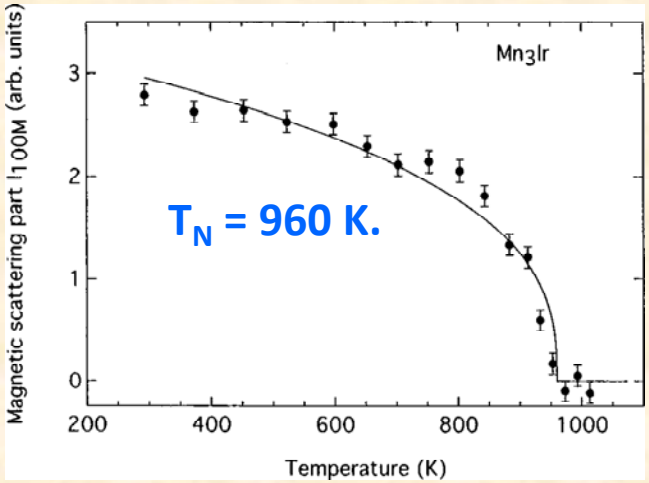

T_N = 960 K.

Very large T_N.

fcc lattice = *ABC* stacked triangular layers ⊥ <111>

It comes in other forms...

Relevant for sputtered thin films.

1. **Disordered $IrMn_3$: 3Q SDW: θ=54.7^0**

2. **Disordered Ir_xMn_{100-x}: 2Q SDW: θ=90^0**

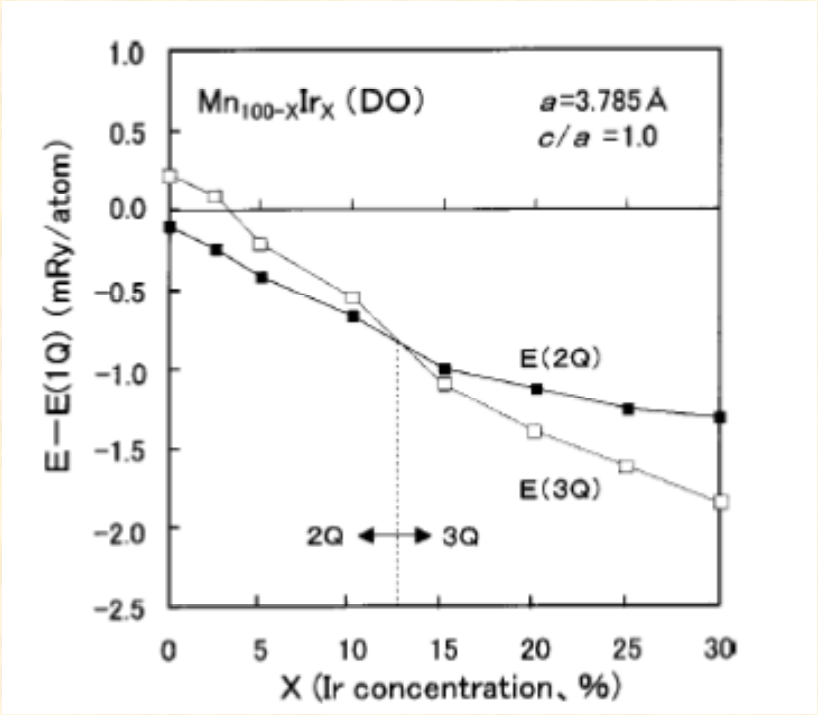

Sakuma *et al*, PRB 67, 024420 (2003).
"First-principles study of the magnetic structures of ordered and disordered Mn-Ir alloys."

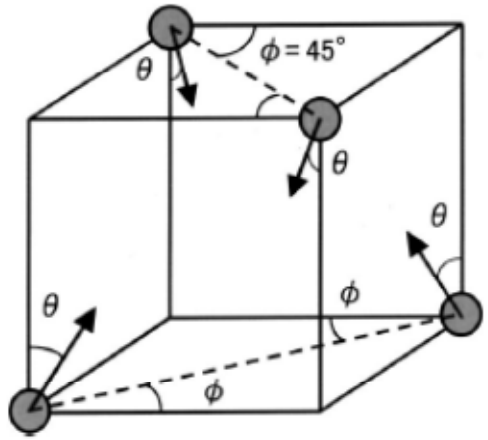

FIG. 3. Multiple-Q spin density wave (MQSDW) structures in the magnetic primitive cell of an fcc lattice.

Ordered $IrMn_3$ $\Longrightarrow$

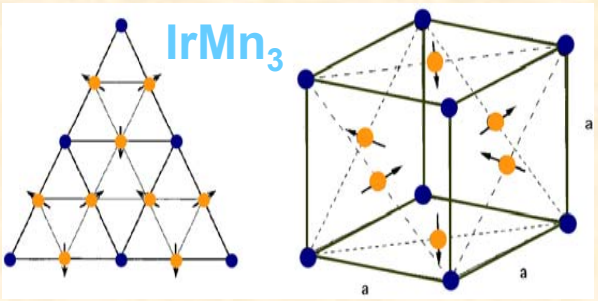

Applied Physics: 'T1' spin structure (no mention of Kagomé).

E. Krén et al, Phys. Lets. 20, 331 (1966).
I. Tomeno et al J. Appl. Phys. 86, 3853 (1999).

Thin films of $IrMn_3$ form <111> planes.

fcc Kagomé lattice = *ABC* stacked Kagomé layers ⊥ <111>

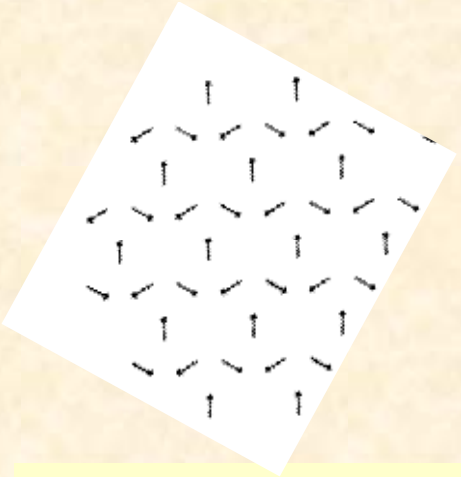

2D Kagomé: Highly Frustrated AF

Basic Physics: 'q=0' spin structure (no mention of 'T1').

A.B. Harris et al, PRB 45, 2899 (1992).

•2D Heisenberg model exhibits coplanar spin structure.

• Macroscopic spin degeneracy at T=0

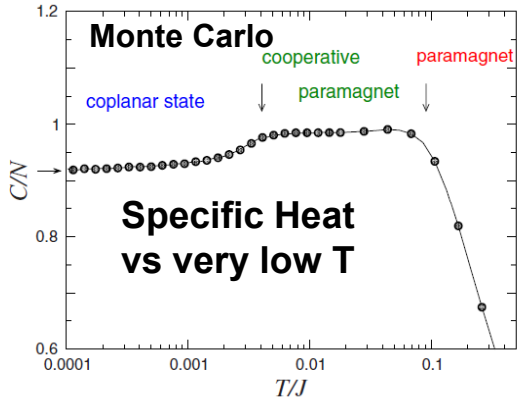

FIG. 3. (Color online) Temperature dependence of the specific heat for a kagome lattice cluster with $L=36$. The horizontal arrow denotes the value $C/N=\frac{11}{12}$. The two vertical arrows indicate boundaries between three different regimes.

M. Zhitomirsky, PRB 78, 094423 (2008).

Monte Carlo simulations of the fcc Kagomé lattice.

Heisenberg and XY Models with NN Exchange J Only.

V. Hemmati, M.L. Plumer, J.P. Whitehead, and B.W. Southern, PRB submitted (2012).

J ⇒ 4 NN in-plane

+ 2 NN above + 2 NN below

ABC stacked **View along <111>**

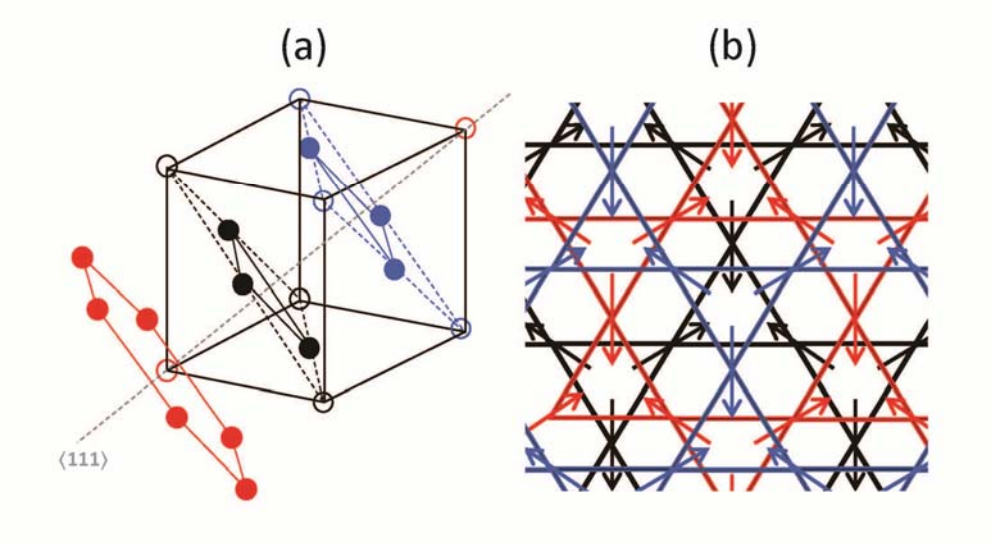

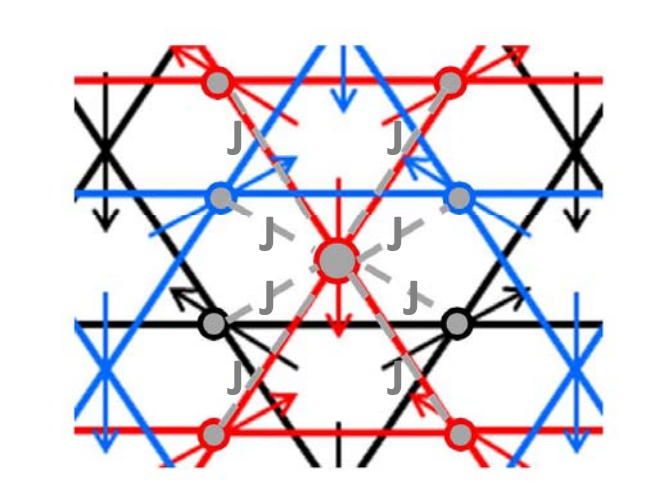

- Recall fcc = ABC stacked triangular layers with 12 NN^s.
- Regular fcc AF with NN Heisenberg exchange shows first order transition to a collinear state.

Ground State from simulations:

- Each layer has q=0 spin structure.
- 120^0 between all 8 NNs.

Monte Carlo simulations of the fcc Kagomé lattice.

Energy and Specific Heat.

- *Standard Metropolis MC.*
- *L* layers of ABC stacked *LxL* Kagomé planes with PBC.
- *L* = 12, 18, 24, 30, 36, 60 with MCS = 10^6 – 10^7
- *Cooling, Heating and Independent* temperature runs.

Energy **L=24** **Specific Heat**

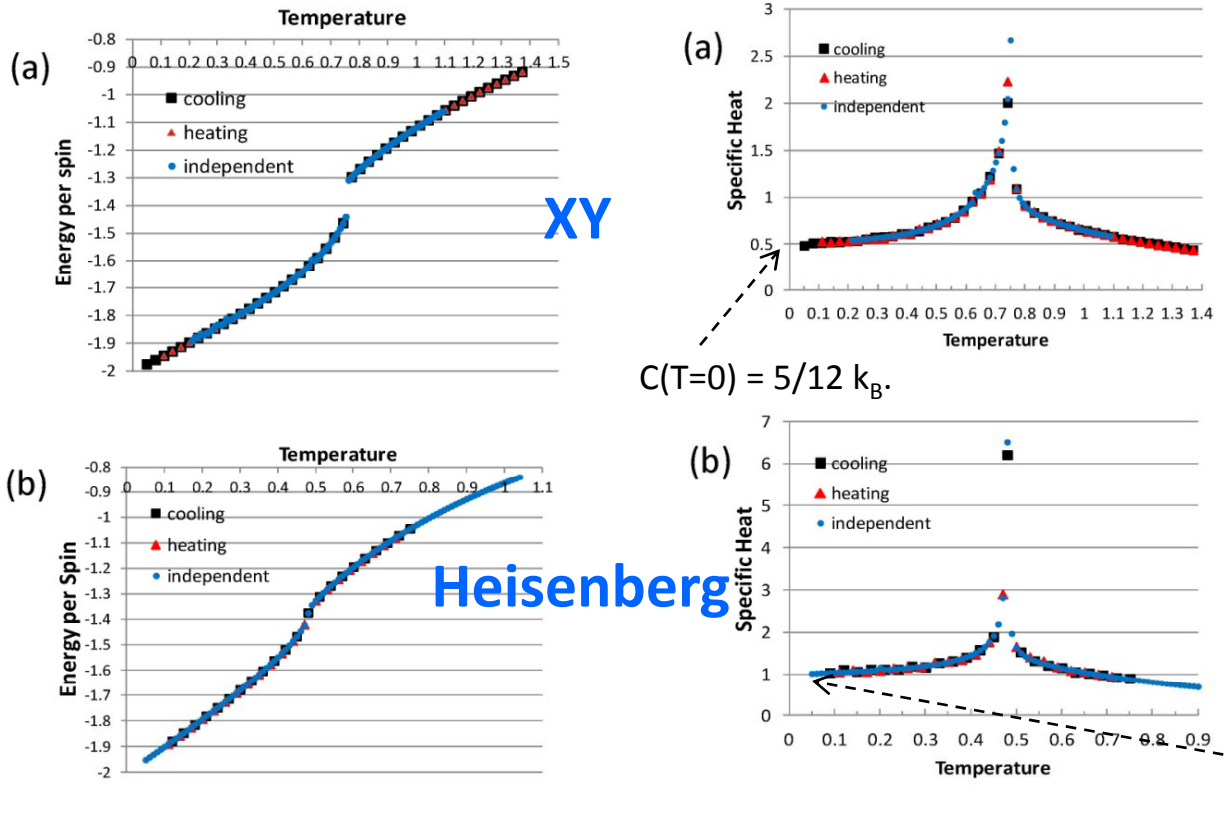

- **All three types of simulations yield equivalent results.**
- **For XY model, T_N = 0.760 and appears to be strongly first order.**
- **For Heisenberg model, T_N = 0.476 and could be first order.**

Monte Carlo simulations of the fcc Kagomé lattice.

Order of the Transitions.

Heisenberg Energy.

L=36.

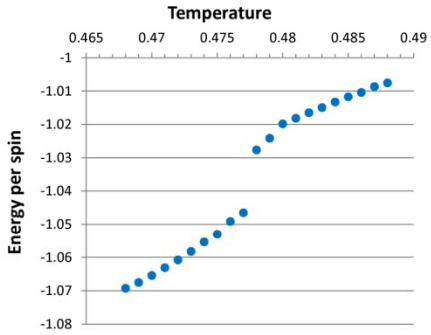

Discontinuity in Heisenberg energy clearer at L=36.

Energy Histograms near T_N

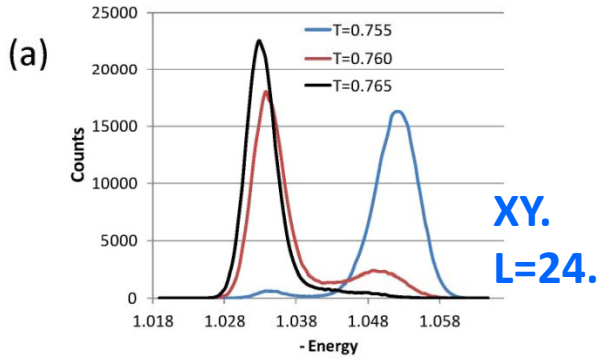

XY.

L=24.

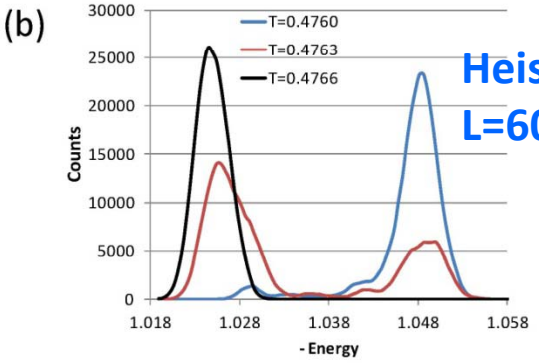

Heisenberg.

L=60.

Indicate energy gap between disordered and ordered phases for *both* models.

Binder *Heisenberg* Energy Cumulant near T_N.

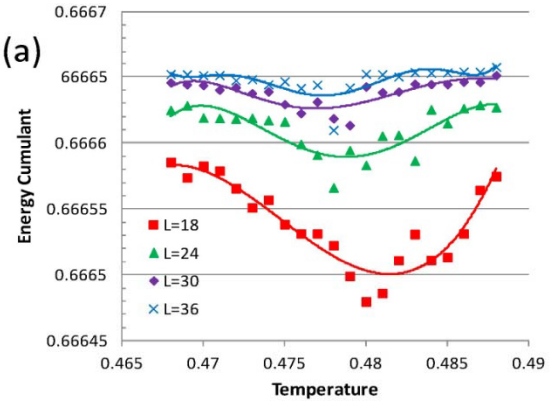

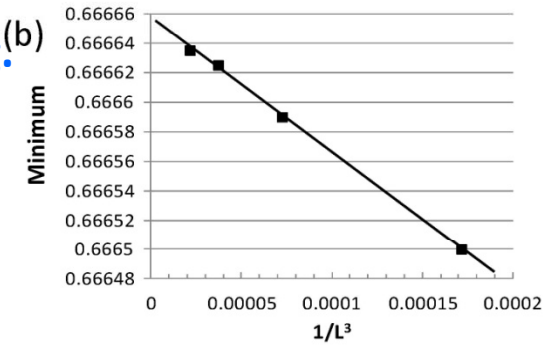

Inconclusive: Could be 2/3, or just close.

Monte Carlo simulations of the fcc Kagomé lattice.

q=0 Order Parameter and Susceptibility.

Order Parameter **L=24** **Susceptibility**

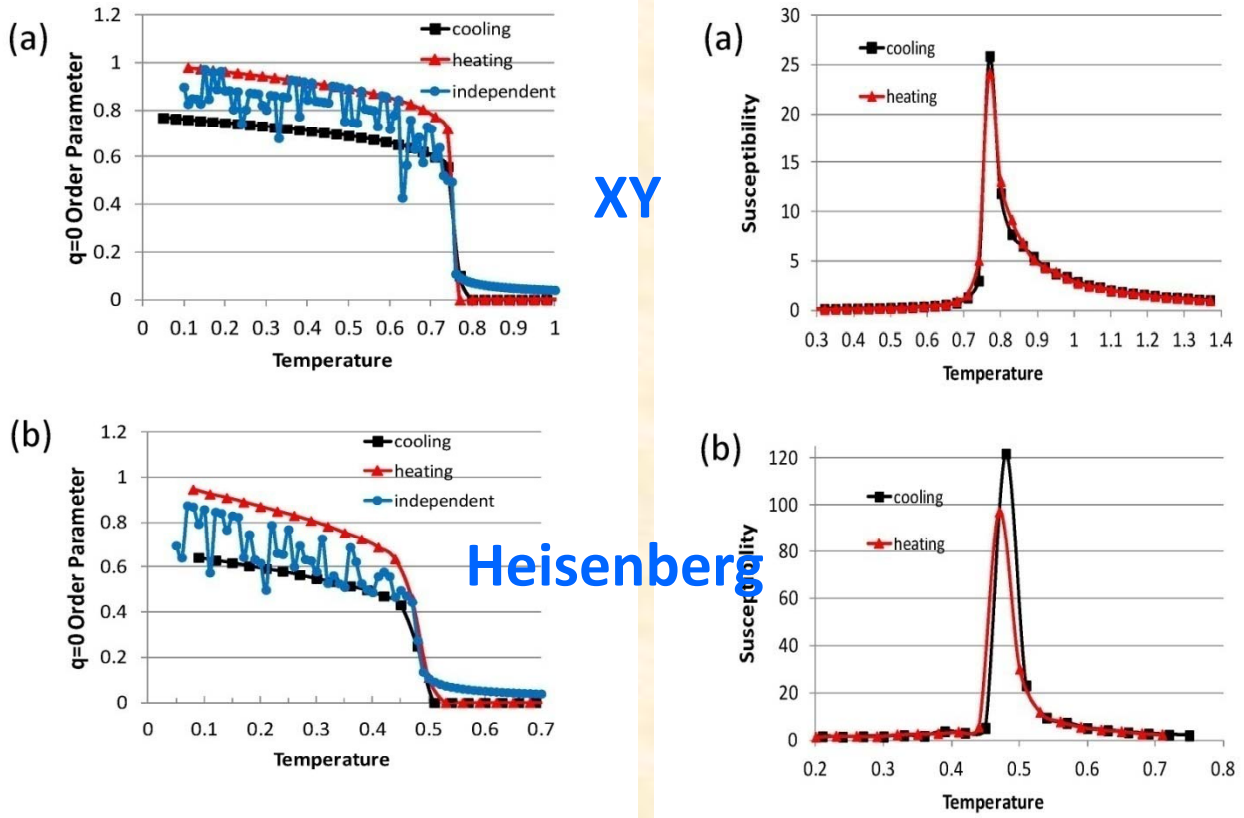

- **Heating runs start at T=0 from fully order q=0 state.**
- **Order Parameter and Susceptibility show strong dependence on simulation mode (heating, cooling or independent temperature) and fluctuates between values, *in contrast with energy and specific heat.***
- **This feature is due to Kagomé-lattice spin degeneracies**

Monte Carlo simulations of the fcc Kagomé lattice.

Spin Degeneracies.

Define 3 ferromagnetic sub-lattice magnetization vectors: black, blue red.

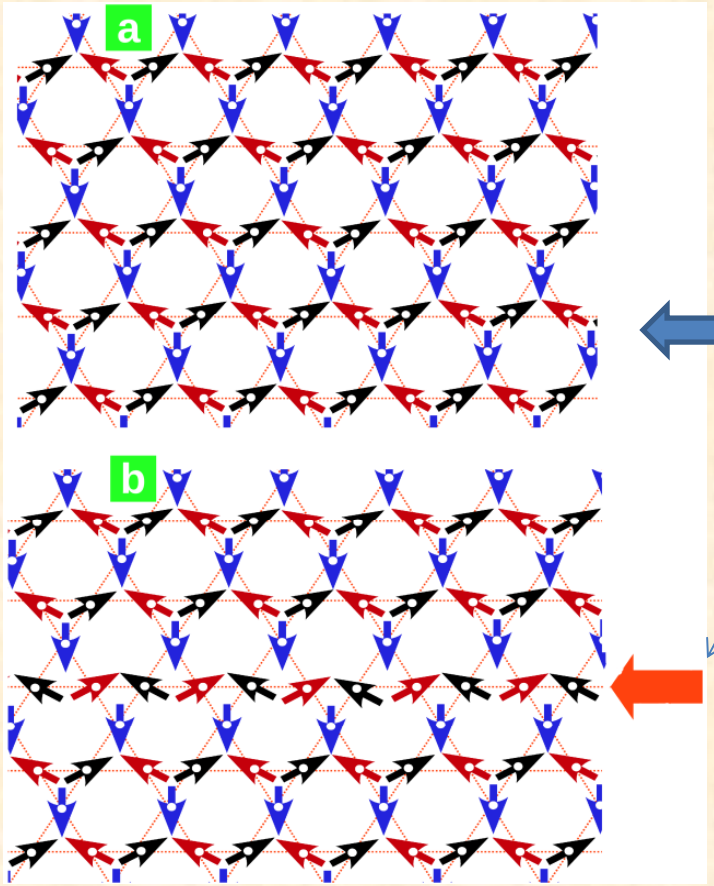

'q=0' magnetic structure ⇒ 3 spins around each triangle at 120^0

In 2D, can switch direction of two of the sub-lattices vectors in a row (e.g., **black** ⟷ **red**) with no change in energy.

In 3D, can switch direction of two of the sub-lattices vectors in a plane with no change in energy

Monte Carlo simulations of the fcc Kagomé lattice.

Spin Degeneracies.

Enumerate all possible switches for L=24 and determine size of ground-state sub-lattice moment:

$$M_\eta = \frac{\sqrt{\left(\frac{1}{4}L^3 - \frac{3}{2}n\right)^2 + \left(\frac{\sqrt{3}}{2}n\right)^2}}{\frac{3}{4}L^3}$$

$L^3/8 \leq n \leq L/2$

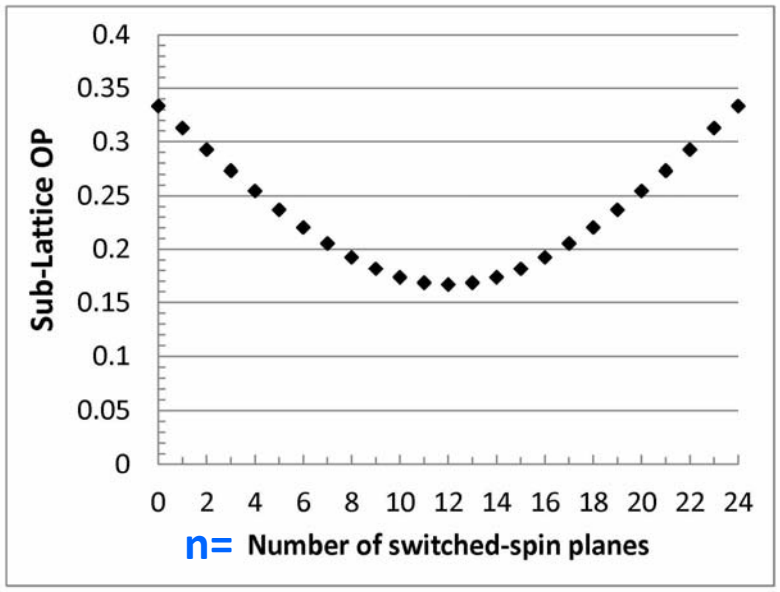

Three different MC cooling runs (different random initial configuration).

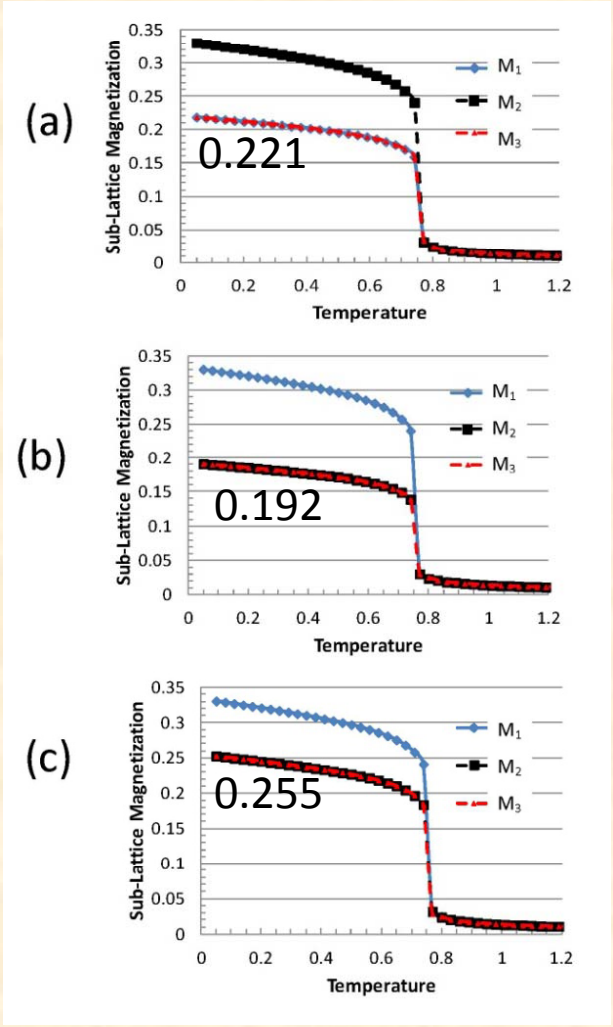

- **One sub-lattice is always fully saturated.**
- **The other two randomly approach (T=0) predicted values.**

Monte Carlo simulations of the fcc Kagomé lattice.

Interlayer coupling J'.

J=1

Set inter-layer to J' < 1.

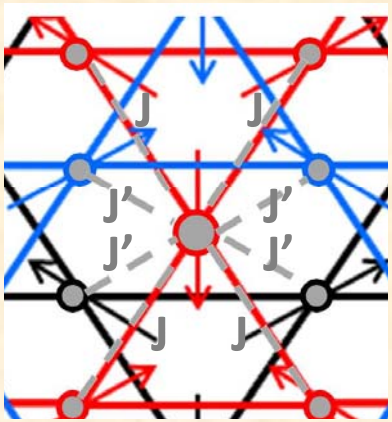

Specific Heat

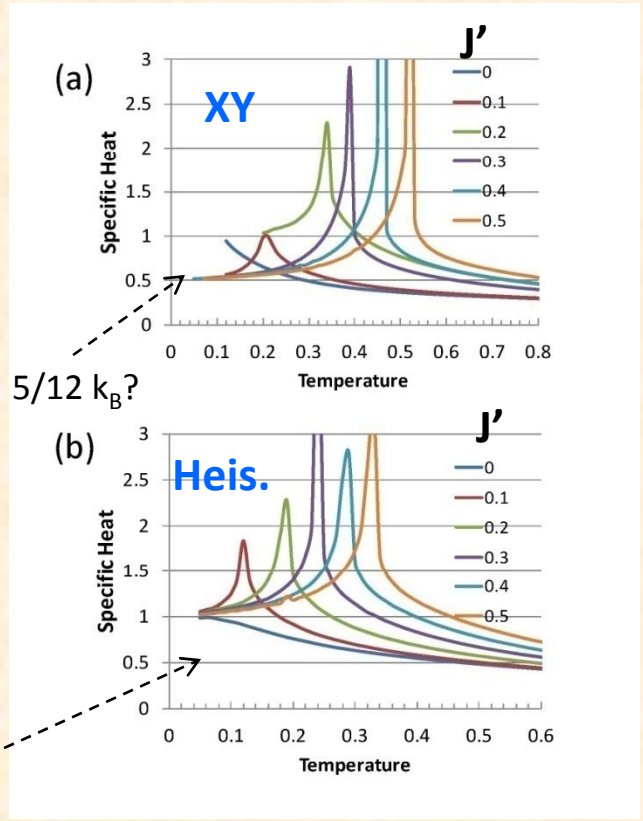

T_N vs J'.

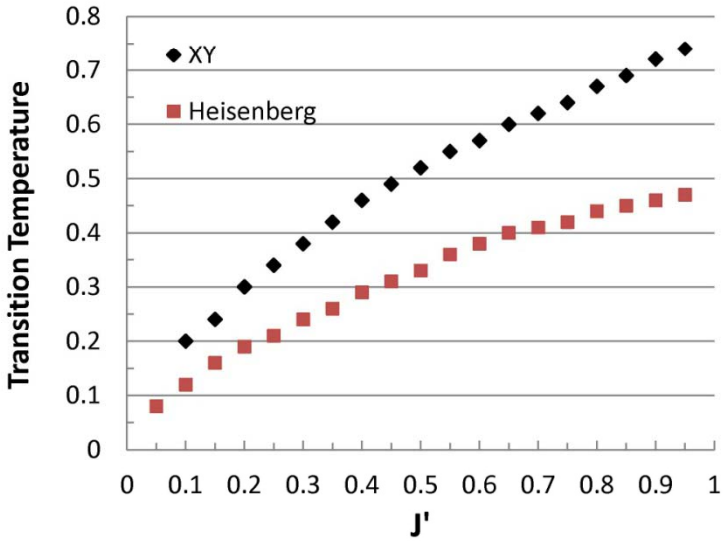

Trends are similar to other quasi 2D systems.

Monte Carlo simulations of the fcc Kagomé lattice.

Add anisotropy

L. Szunyogh et al PRB 79, 020403 (2009)

$$H = -\frac{1}{2}\sum_{i\neq j} J_{ij}\vec{S}_i\vec{S}_j - \frac{K_{\text{eff}}}{2}\sum_i (\vec{S}_i\cdot\vec{n}_i)^2,$$

Effective local anisotropy axes (similar to spin-ice pyrochlore tetrahedrons).

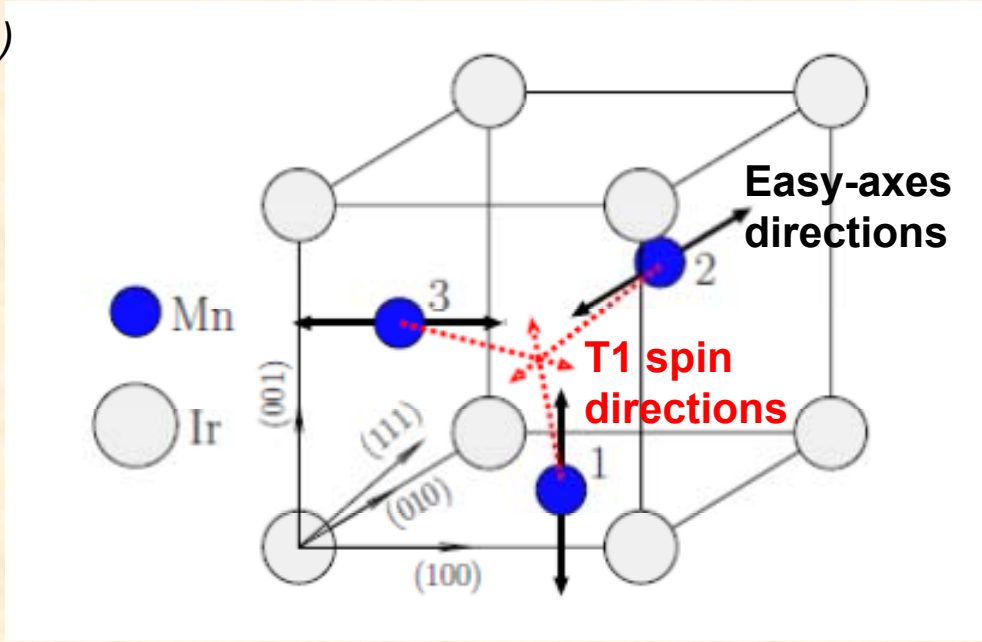

Mn moments are *not* aligned in the easy-axes directions for the coplanar T1 spin structure.

Work in progress.

Relation to Exchange Pinning.

DFT calculations of $IrMn_3/CO_4$ and $IrMn_3/Fe_4$ interface spin structures. *H. Takahashi et al, J. Appl. Phys. 110, 123920 (2011)*

Interaction with ferromagnetic layer induces a net moment in surface Mn spins

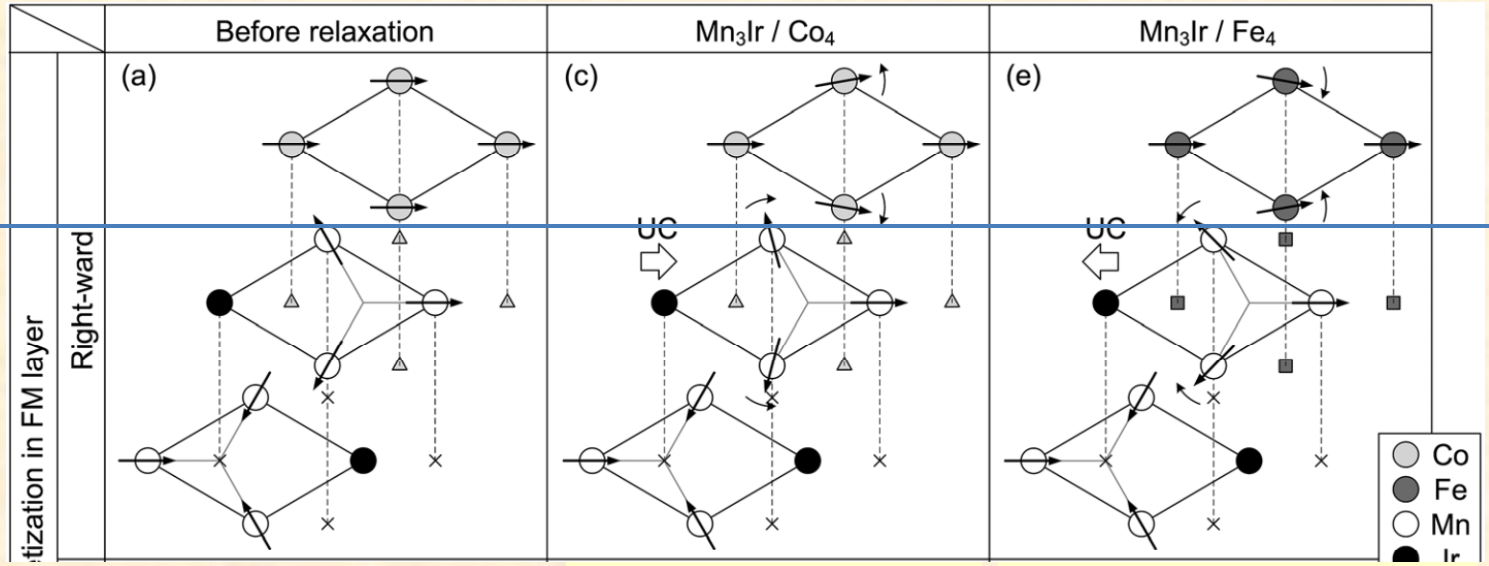

Mn moments rotate toward Co-moments

Mn moments rotate away from Fe-moments

Relation to exchange pinning?

A Model of Exchange Pinning

Domains **involving non-magnetic surface sites.**

Relevant for $IrMn_3$?

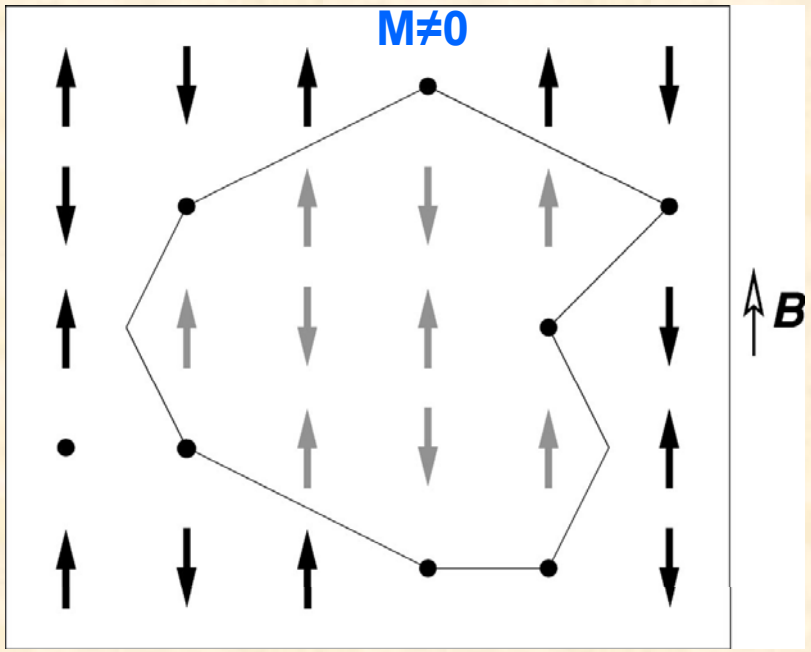

U. Nowak et al PRB 66, 014430 (2002).

M. R. Fitzsimmons et al, PRB 77, 224406 (2008).

Phase transitions in the fcc Kagomé lattice

Summary and Conclusions

• 3D fcc Kagomé lattice with NN exchange only shows LRO transitions of the 'q=0' type at T_N=0.760 J for the XY model and T_N = 0.476 J for the Heisenberg model.

• XY model ⇒ Strongly first order.
• Heisenberg model ⇒ Probably weakly first order.
• Mean field theory ⇒ Continuous transition in both cases.

• Spin degeneracies of the 2D model persist in the 3D case ⇒ Order-by-disorder?

Future work:
- effects of anisotropy.
- thin films and surface effects
- add a ferromagnetic layer and dipole interactions.
- ⇒ ***Exchange Pinning?***

Evidence for first-order transition in $IrMn_3$: χ vs T

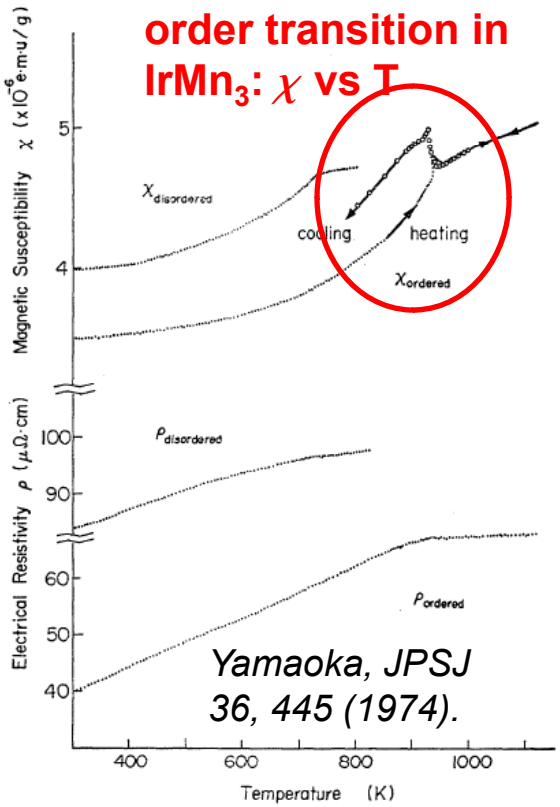

Fig. 5. Temperature dependences of magnetic susceptibility χ and electrical resistivity ρ of the partially ordered (S=0.83) alloy compared with those of the disordered (S<0.08) alloy with x=0.256. Open circles indicate the cooling process.

Magnetic recording, and phase transitions in the fcc Kagomé lattice:

Collaborations and Support: Who's doing the work and who's paying for it.

- **Vahid Hemmati (MSc graduate)** Memorial
- **Jason Mercer (PhD student)** Memorial
- **Martin Leblanc (PhD student)** Memorial
- **Tim Fal (postdoc)** Memorial
- **John Whitehead (professor)** Memorial
- **Byron Southern (professor)** U. of Manitoba
- **Johannes Van Ek (physicist)** Western Digital Corporation

- **Natural Sciences and Engineering Council of Canada**
- **Western Digital Corporation**
- **Canada Foundation for Innovation**
- **Atlantic Centre of Excellence Network**

Grain Size Progression vs. Areal Density

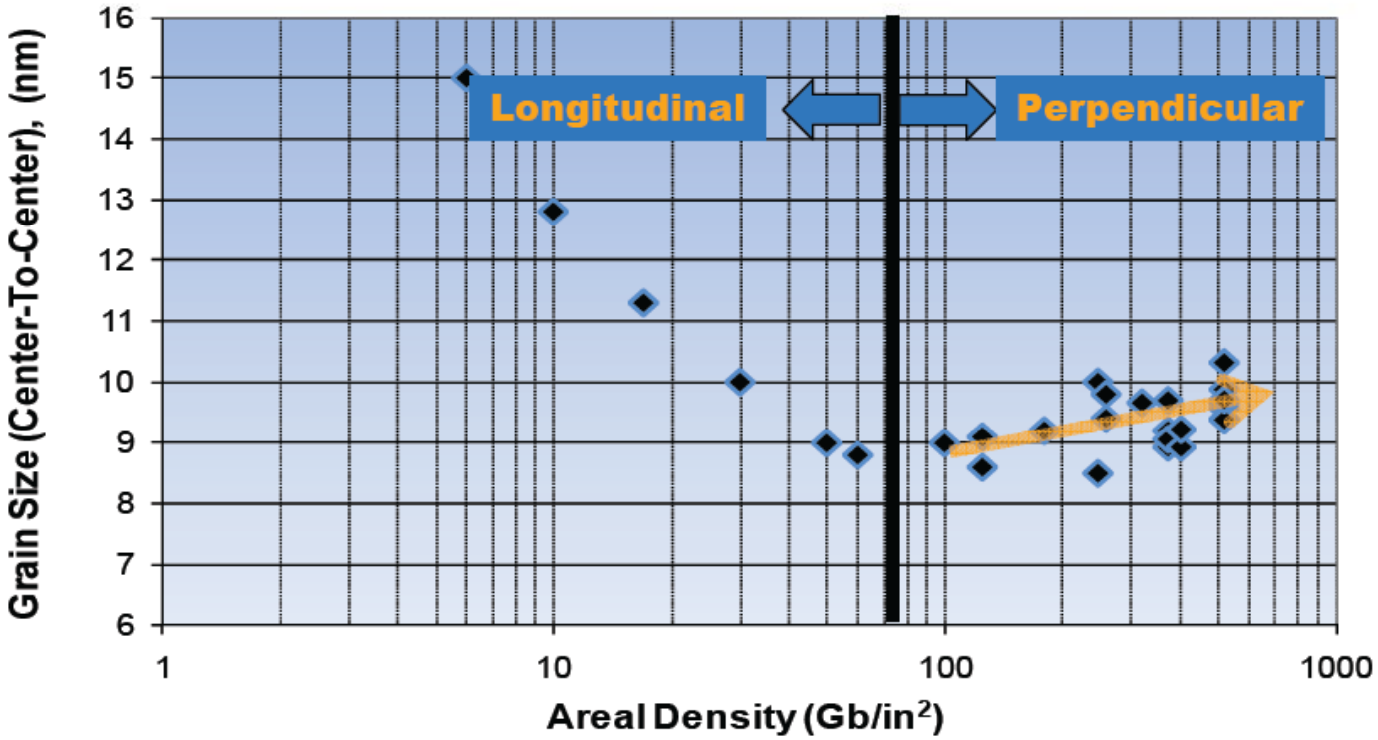

- ECC media structure was expected yield higher areal density capability by enabling smaller grain size in media.
- In practice, grain size has remained practically unchanged since PMR introduction.
- Instead, the trade-off of choice was to use ECC media to improve writability, maintain acceptable adjacent track erasure, and optimize transition parameter with utilization of higher Ku alloys and optimization of lateral exchange coupling through the various layers.

Monte Carlo simulations of the fcc Kagomé lattice.

V. HEMATTI, M.L. PLUMER, J.P. WHITEHEAD, Memorial University of Newfoundland,
B.W. SOUTHERN, University of Manitoba

http://www.mun.ca/physics/
http://www.physics.umanitoba.ca/

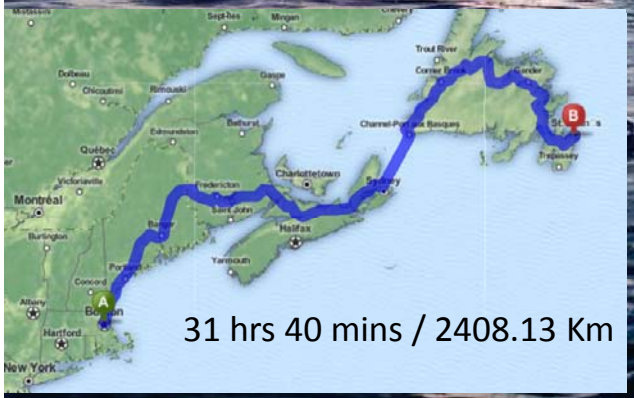

Finite Element Method: *Magsoft*

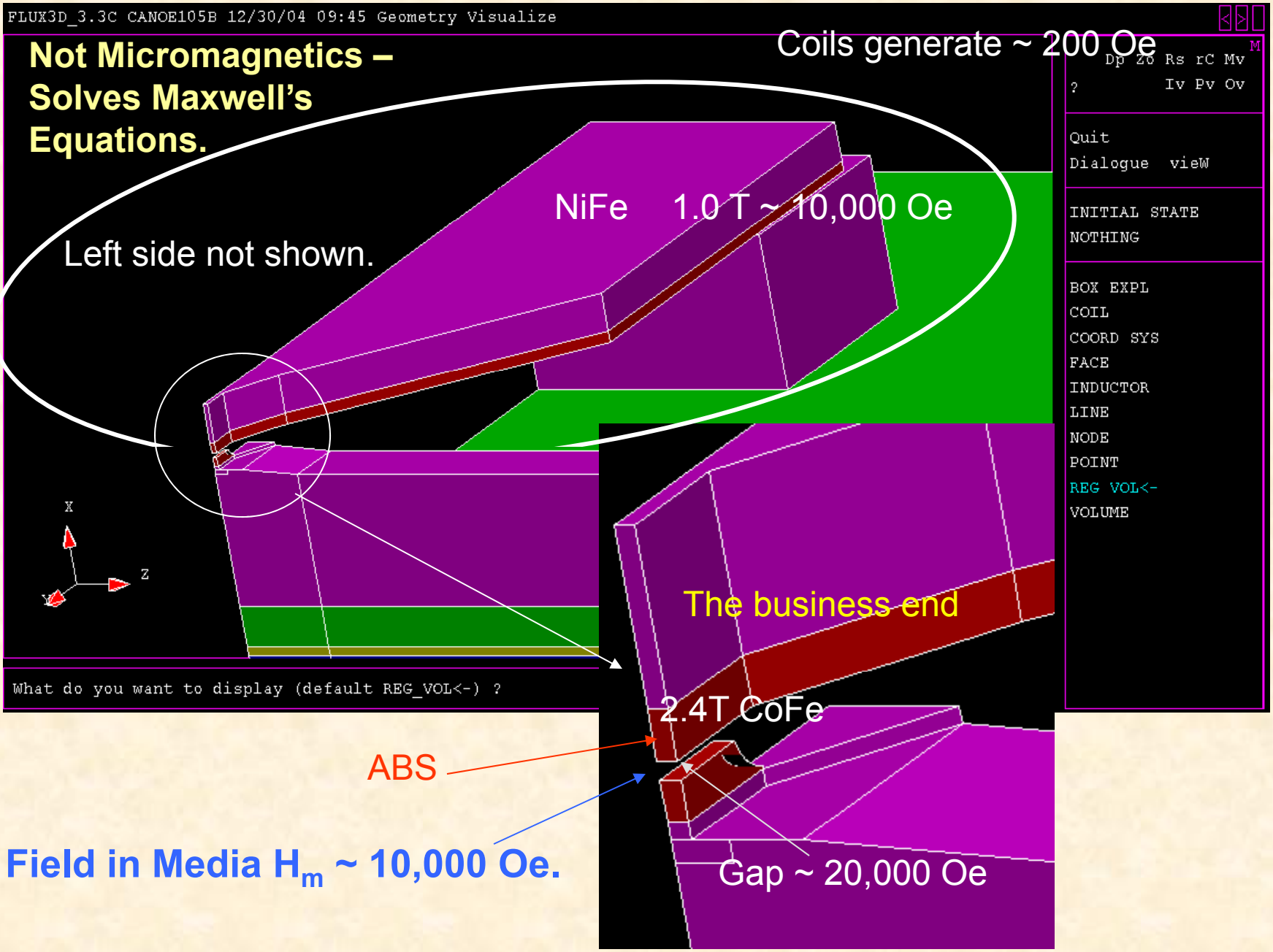

X-section and ABS view of an Integrated MR Head

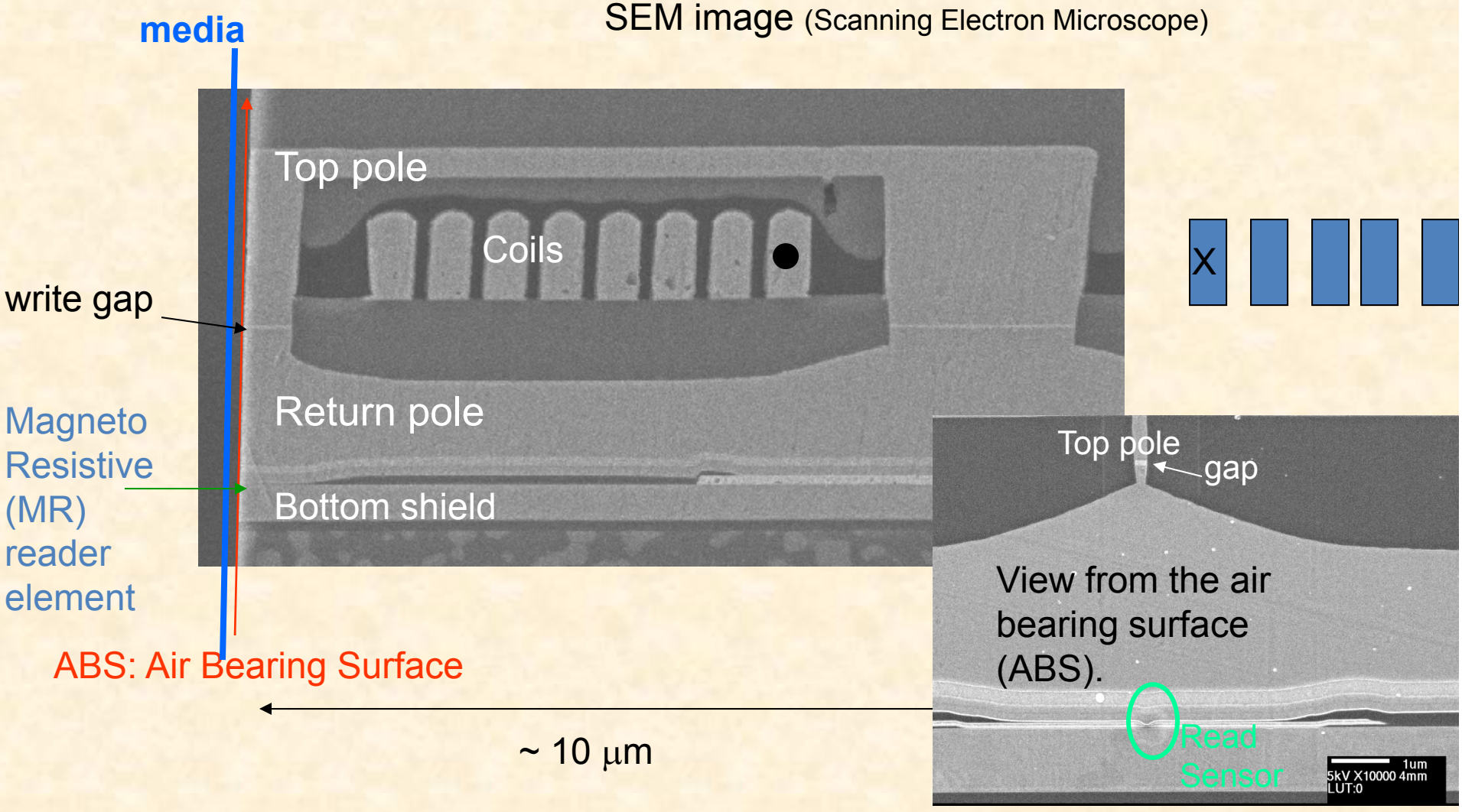

The Media: A model of granular recording media

Cobalt Atoms ⇒ Hexagonal Crystal Structure: *High Anisotropy*

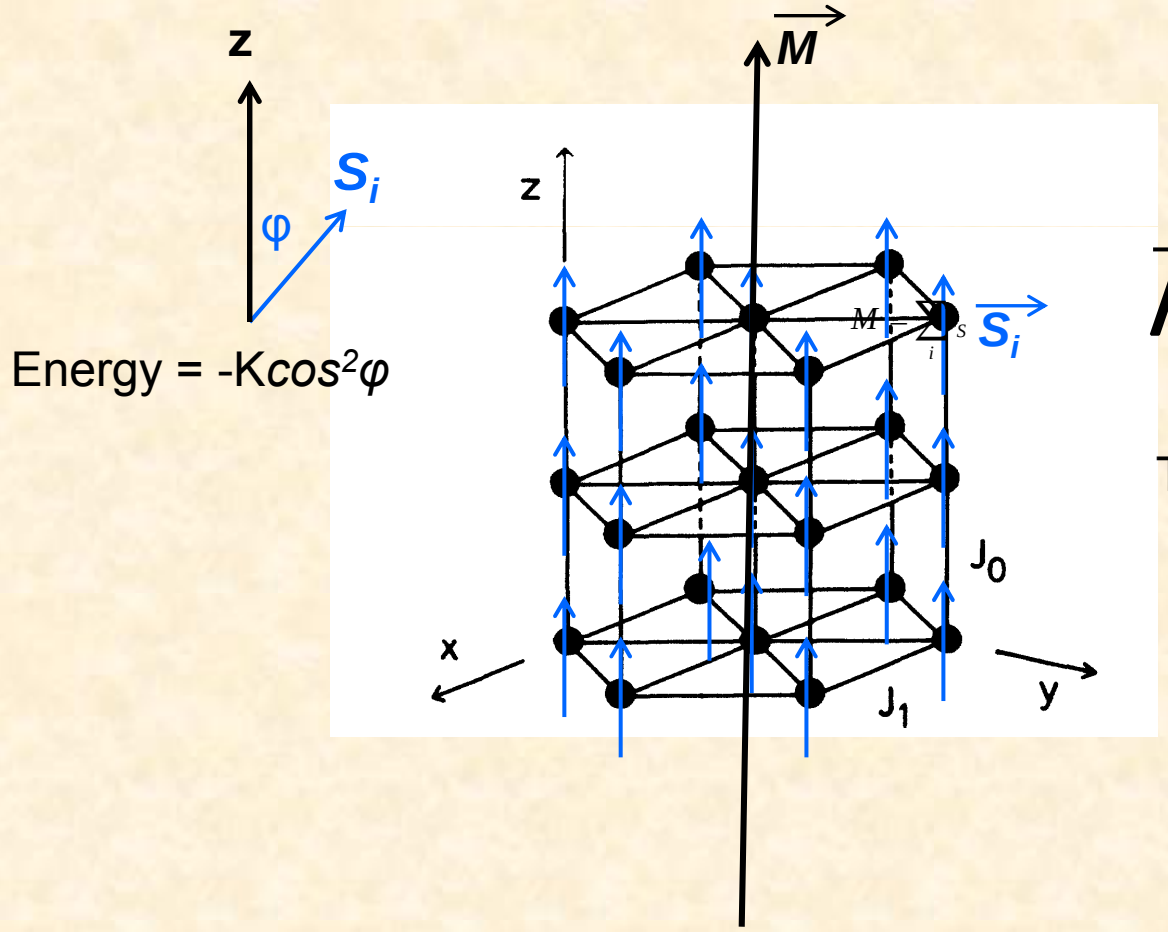

1000s of Atomic spins

$$\vec{M} = \sum_i \vec{S}_i$$

Total magnetization

Anisotropy
$\Rightarrow \vec{M} \parallel \hat{z}$

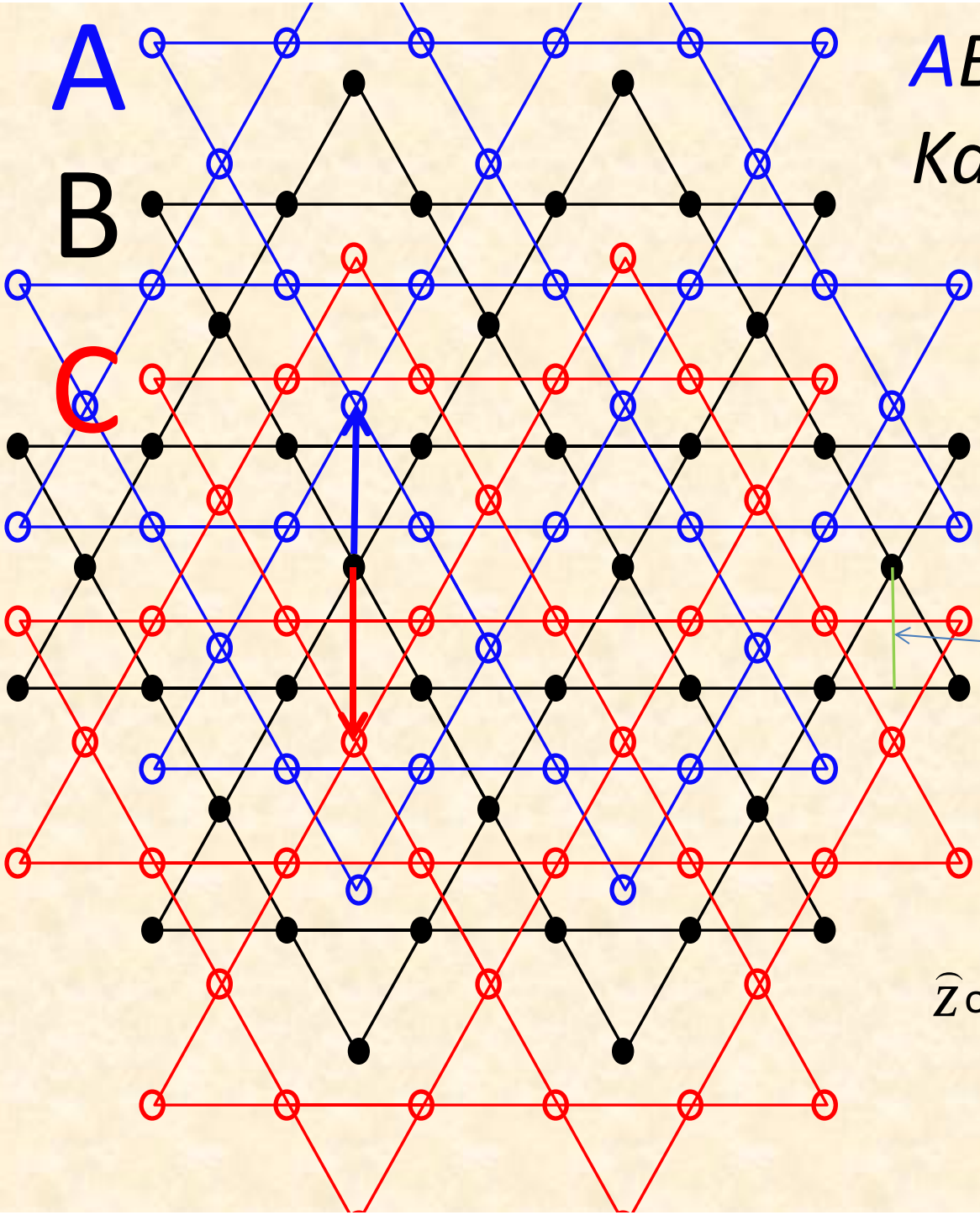

ABC stacked Kagomé

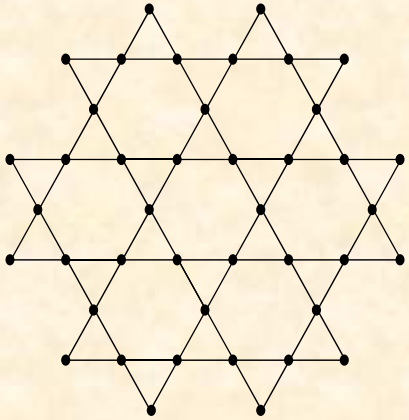

$b = (\sqrt{3}/2)a$

$w = \frac{4}{3} b\hat{y} + \frac{1}{3} c\hat{z}$

$w = -\frac{4}{3} b\hat{y} - \frac{1}{3} c\hat{z}$

$\hat{z}$ out of page, along <111>

Ferromagnets: Cannot ignore "magnetostatic" fields.

$$\vec{H}(\vec{r}) = -\int_V d\tau \frac{\vec{\nabla}\cdot\vec{M}(\vec{r}')(\vec{r}-\vec{r}')}{|\vec{r}-\vec{r}'|^3} + \int_S dA \frac{\hat{n}(\vec{r}')\cdot\vec{M}(\vec{r}')(\vec{r}-\vec{r}')}{|\vec{r}-\vec{r}'|^3}$$

Long range interaction ~ $1/r^3$

For grains of finite size, it's not just dipole-dipole

Increases computational demands.

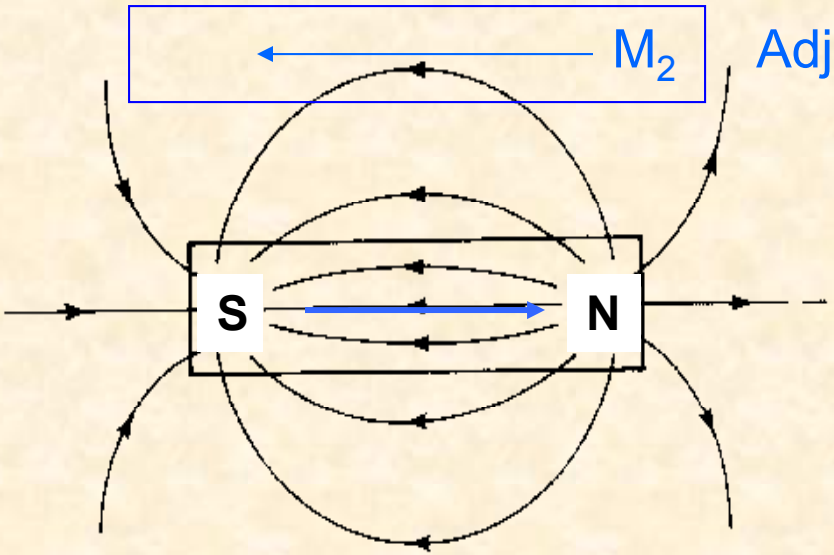

Adjacent bar magnet lies anti-parallel

- **Outside of bar M=0; H = B = stray field**
- **Inside of bar B = H + 4 π M_r, 'demagnetizing' field H opposes M**

Landau-Lifschitz-Gilbert Equation

Precession and phenomenological damping:

Torque Equation

$$\frac{d\vec{M}}{dt} = -\gamma \vec{M} \times \vec{H}$$

Add damping

$$\vec{H}(\vec{r},t) \rightarrow \vec{H}_{\text{eff}}(\vec{r},t) - \eta \frac{d\vec{M}(\vec{r},t)}{dt}$$

LLG:

$$(1+\alpha^2)\frac{d\vec{M}}{dt} = -\gamma \vec{M} \times \vec{H}_{eff} - \frac{\alpha\gamma}{M}\vec{M} \times \left(\vec{M} \times \vec{H}_{eff}\right)$$

$\alpha = \eta\gamma M$

$$\vec{H}_{effective} = \vec{H}_{applied} + \vec{H}_{anisotropy} + \vec{H}_{exchange} + \vec{H}_{magnetostatic}$$

Not just dipole

Norm conserving:

$$\frac{d\left|\vec{M}\right|^2}{dt} = 2\vec{M} \cdot \frac{d\vec{M}}{dt} = 0$$

$$\vec{a} \cdot (\vec{a} \times \vec{b}) \equiv 0$$

$\alpha \sim 0.1 - 0.001$

Spin-wave interactions, magnetoelastic coupling, impurities,…

Modeling (Simulations) to the Rescue.

Micromagnetics of Ferromagnets: Interacting, ***uniformly magnetized grains.***

Thin ferromagnetic films with small shapes and big demagnetization (magnetostatic) fields at edges.

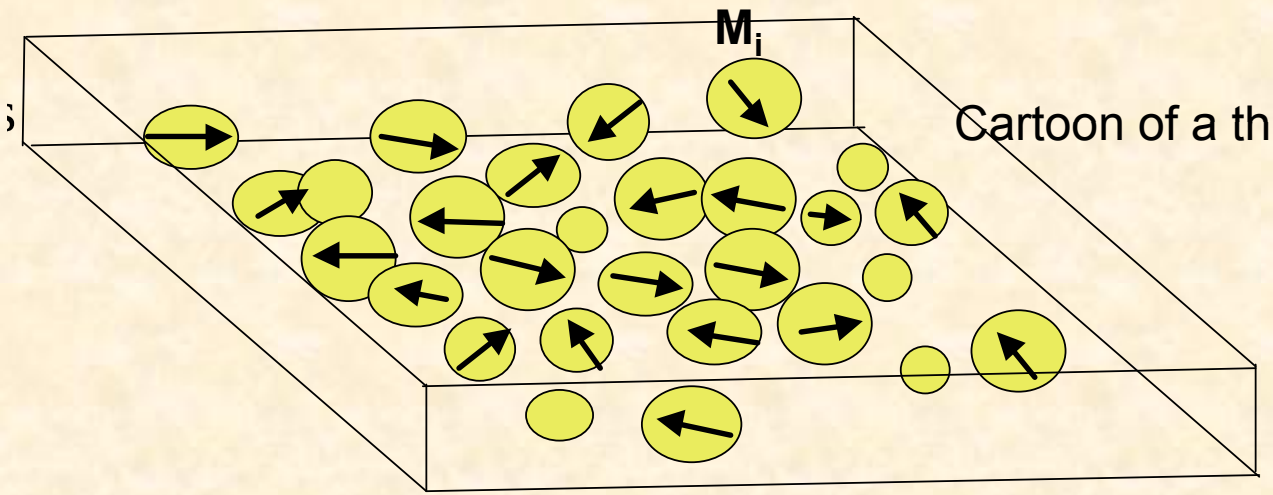

Cartoon of a thin film

Grain size ~ 8 nm ⇒ 1000's of atoms.

Patterned Devices: Shape Anisotropy

- Series of solutions for platelets with different aspect ratios: what do we see?
  - CoFe, 2.5 nm thick, 10 nm cells (single layer)

Micromagnetic Modeling

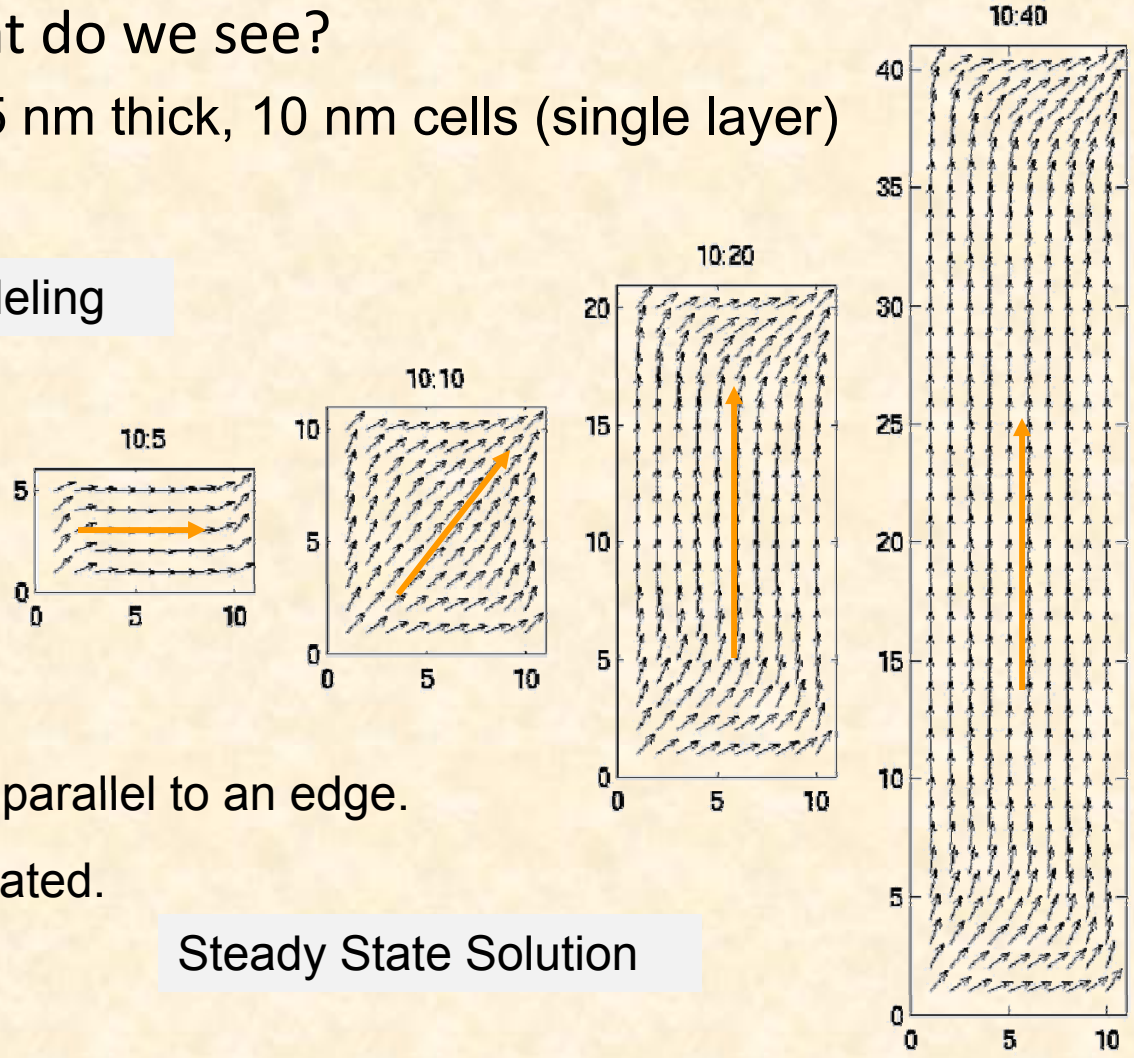

•Moments tend to lie parallel to an edge.

•Corners are complicated.

Steady State Solution

A model...

No obvious mechanism for exchange pinning from compensated surface (M=0).

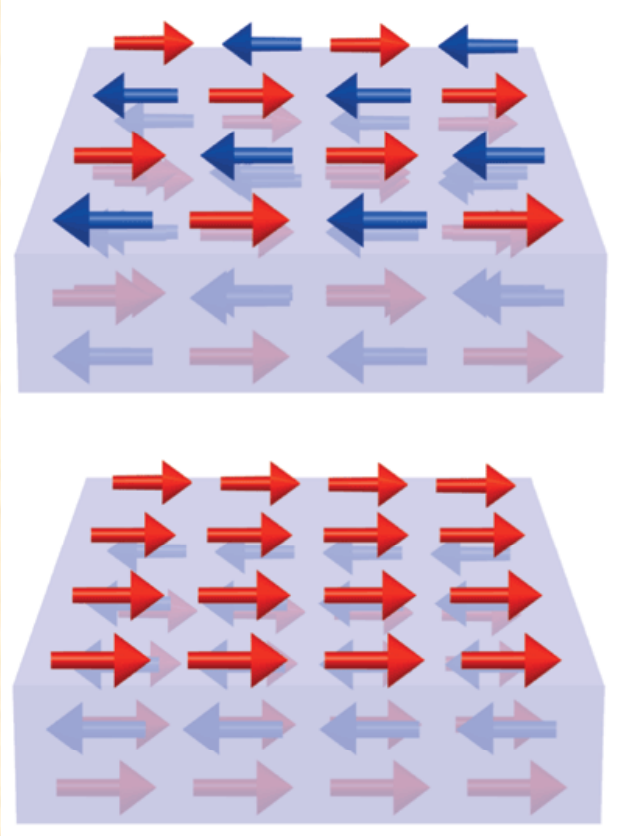

The atomic-scale *Roughness* can create uncompensated spins (red)

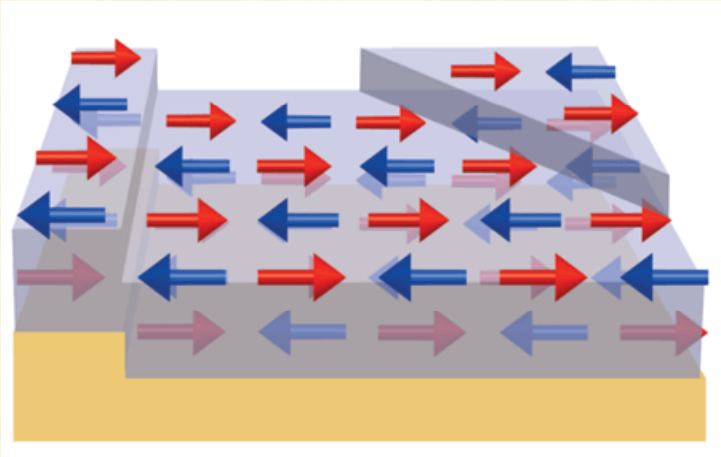

M. Blamire and B. Hickey, Nature Mater. 5, 87 (2006).

J. Spray and U. Nowak, J. Phys. D 39, 4536 (2006).

Exchange Pinning in Spin Valves

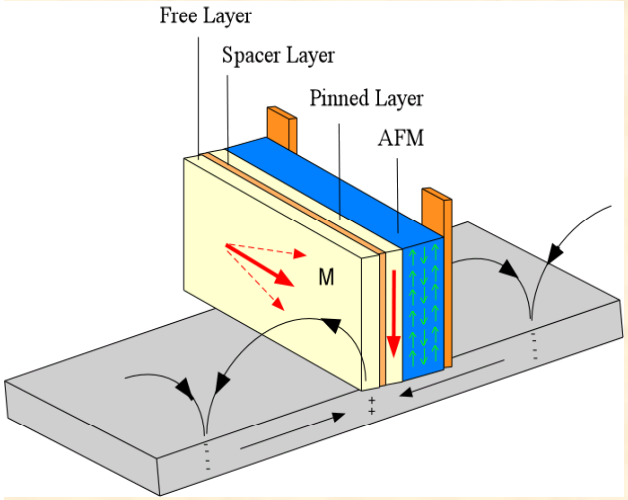

- **Pins the Pinned Layer so it does not respond to media bit transition fields.**
- **Requires T_N >> drive operating temperatures~ 350 K.**

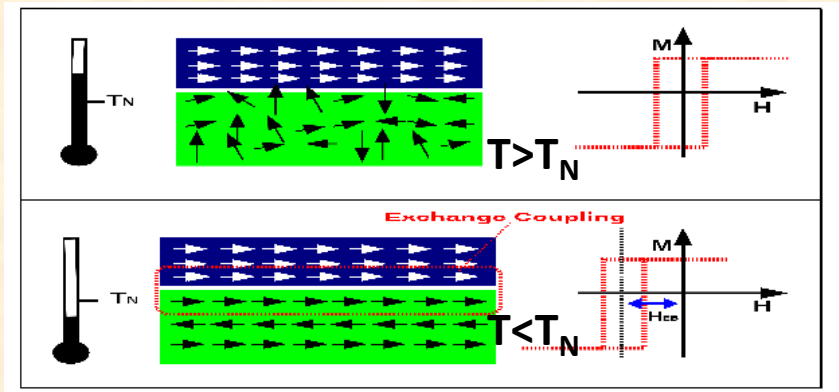

Field cooling to obtain exchange bias.

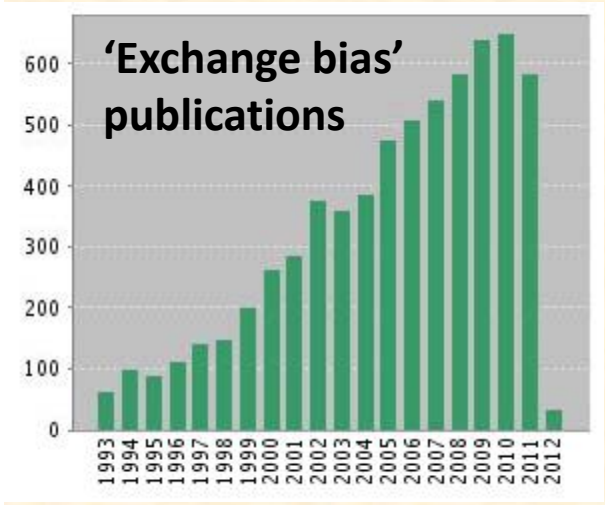

- **Surface spin structure in AF results in a small ferromagentic moment.**
- **Induces a *uni-directional* field on the PL.**
- **"After more than 50 years there is still no definitive theory that can account for the observed effects.." K. O'Grady et al., JMMM 322, 883 (2010).**

H. Takahashi et al, J. Appl. Phys. 110, 123920 (2011)

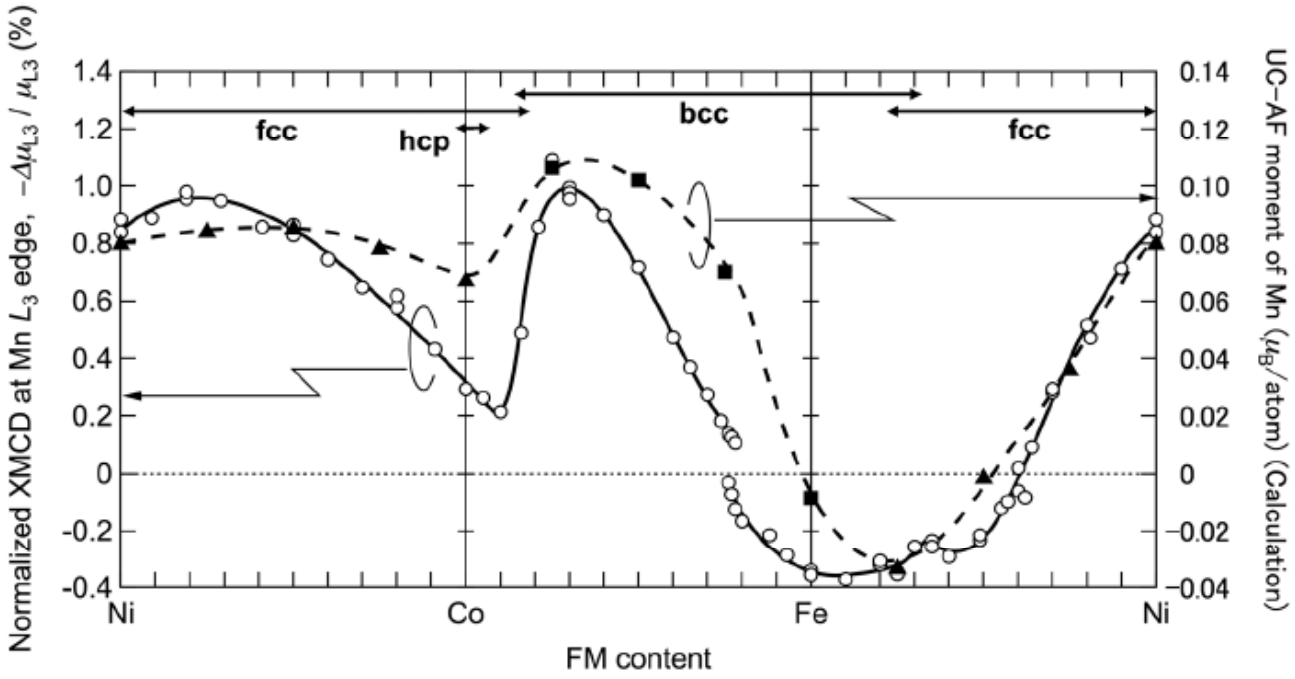

FIG. 8. Comparison of the experimental and calculation results for the net magnetic moments in the Mn-Ir/(Ni-Co, Co-Fe, Fe-Ni) bilayer system. The circle marks represent the experimental results. As the calculation results, the bcc structure (triangle marks) was employed for Co_3Fe_1, Co_2Fe_2, and Co_1Fe_3, Fe_4, and the fcc structure (square marks) was employed for the other compositions. This facilitated comparison with the results of the experimental analysis.